LTE 系統下感知式 Femtocell 之優先次序資源管理機制

A Priority-based Resource Management Scheme for Cognitive Femtocell in LTE System

研 究 生：葉長青　　Student：Chang-Cing Ye

指導教授：張仲儒 博士　　Advisor：Dr. Chung-Ju Chang

國立交通大學

電信工程研究所

碩士論文

A Thesis

Submitted to Institute of Communication Engineering

College of Electrical and Computer Engineering

National Chiao Tung University

in Partial Fulfillment of the Requirements

for the Degree of Master of Science

in

Communication Engineering

July 2012

Hsinchu, Taiwan

中華民國 一０一 年 七 月

LTE 系統下感知式 Femtocell 之
優先次序資源管理機制

研究生：葉長青　　指導教授：張仲儒 博士

國立交通大學電信工程研究所

摘要

由於宏細胞(macrocell)無法提供足夠的服務給室內用戶，家庭基站(femtocell)被提出來改善室內用戶的服務效能。然而，家庭基站的佈建會對宏細胞系統造成無法預期的感擾，並降低周遭室外用戶的服務效能。為了解決這個難題，混合式接取技術被視為一個大有可為的解決方法。混合式接取技術使家庭基站能夠去服務周遭的室外用戶，並卸載宏細胞的電信業務。

在本篇論文中，我們提出感知優先次序資源分配(cognitive priority-based resource management, CPRM)機制，意圖最大化感知式家庭基站的傳輸量，並保證滿足各種電信業務的服務品質要求。CPRM 機制會動態調整感測時間以達到準確的感測結果、設計優先次序來表明用戶需要服務的緊急程度、決定用戶的最小傳輸位元數來滿足用戶的服務品質要求。然後，CPRM 機制會依照優先次序分配資源以避免違反緊急用戶的服務品質要求。模擬結果顯示我們提出的 CPRM 機制能達到比傳統機制高的系統傳輸量，並保證滿足各種電信業務的服務品質需求。

A Priority-based Resource Management Scheme for Cognitive Femtocell in LTE System

Student: Chang-Cing Ye Advisor: Dr. Chung-Ju Chang

Institute of Communication Engineering
National Chiao Tung University

English Abstract

Abstract

Since macrocells cannot provide enough services to indoor users, femtocell is proposed to improve the service performance of indoor users. However, the deployment of femtocell would cause unexpected interference to the macrocell system, and degrade the performance of the nearby outdoor users. To overcome this challenge, hybrid access policy is envisioned as a promising solution. Hybrid access policy enables femtocell to serve the nearby outdoor users and offload the traffic of macrocell system.

In this thesis, we propose a cognitive priority-based resource management (CPRM) scheme to maximize the throughput of cognitive femtocells with guaranteeing the quality-of-service (QoS) requirements of all traffic types. The CPRM scheme adapts the sensing duration to achieve accurate sensing result, designs the priority function to indicate the degree of urgency of users, and determines the minimum transmission bits to satisfy the QoS requirements of each user. Then, the CPRM scheme would allocate resource based on the priority to avoid violating the QoS requirements of urgent users. Simulation results show that the proposed CPRM scheme achieves higher system throughput than the conventional schemes with guaranteeing the QoS requirements of all traffic types.

Acknowledgement

誌 謝

這篇碩士論文的完成，必須感謝非常多人的幫助與鼓勵。首先要感謝張仲儒教授這兩年多來在專業知識、待人處世與人生規劃上的悉心指導，讓我在學業和生活上都獲益良多。除此之外，還要感謝文敬學長不遲辛勞地給予指導及督促。感謝聖章、耀興、振宇、益興學長們，在我研究上遇到困難的時候，能夠提供我寶貴的意見。還有在進實驗室時熱情歡迎我們的學長，苡仲、俊魁和竣威。當然，還要感謝和我一起努力的同學們，佩珊、恆皜、兼源、莫瑞，以及辛苦的助理玉棋、佳婷。有你們的陪伴，研究的路途多了很多的歡笑。祝福實驗室的大家，學業都能順利，畢業後一帆風順。

最後，我要感謝我最摯愛的父母、兄弟，以及所有關心我、陪伴我、支持我的親友們，他們對我的支持，使我有動力完成碩士的學業。

葉長青 謹誌

民國一０一年七月

Contents

List of Figures

List of Tables

Chapter 1

Introduction

1.1 Motivation

With the development of wireless communication techniques, the wireless communication networks have integrated into our daily life and changed our life style in depth. In order to support a large number of multimedia services, the fourth generation (4G) wireless communication technique was developed from the 3G wireless communication technique [1]-[3]. Among 4G wireless communication standards, long term evolution - advanced (LTE-A) has caught lots of attention, and becomes the main- stream in the development of 4G wireless communication network [4], [5]. The LTE-A system adopts orthogonal frequency division multiple access (OFDMA) technique to provide the degree of freedom in the exploitation of time-frequency resource units. Therefore, it can achieve better resource efficiency, mitigate the inter- or intra-cell interference, and achieve high signal-to-interference-and-noise-ratio (SINR) [5]-[7]. However, due to the penetration loss of walls, the indoor user usually has poor SINR and thus cannot obtain the enough service. As a result, enhancing the received signal quality of indoor users is still an important issue for the LTE-A system.

Femtocell is a promising technique proposed for enlarging the indoor coverage and thus improving the performance of indoor users. Femtocell is a low-power, low-cost, and small-area base station. In the LTE-A system, the femtocell base station

is also called HeNB (home enhanced Node-B or home evolved Node-B). It can connect to the operator's cellular network by the broadband network or the digital subscriber line (DSL), and transmit data with the internet protocol (IP) technique. For the operator, the deployment of femtocell can extend the indoor coverage, increase the spectral utilization, lower the power consumption, and enhance the transmission efficiency and reliability in the macrocell network [8], [9].

Since there is wireless fidelity (Wi-Fi) technology utilized for indoor communication, the comparison between femtocell and Wi-Fi is discussed [10]. Due to the fact that femtocell is operated on the licensed frequency bands, and Wi-Fi is operated on the un-licensed ones, femtocell can achieve better voice quality and securer services than Wi-Fi. Because femtocell is the extension cellular network, it manages service and QoS more efficiently than Wi-Fi, and also it consumes less power than Wi-Fi. Moreover, femtocell is compatible to the existing cellular networks, so it enables seamless handover between macrocell network and femtocell network, while Wi-Fi needs additional handover trigger to switch between different networks.

The access policy of femtocell can be categorized into open access, closed access, and hybrid access [11], [12]. The open access policy indicates that all user equipments (UEs), included home UEs (HUEs) and macro UEs (MUEs), are allowed to connect to HeNB. Thus, the open access policy can improve the overall throughput of network, since MUEs could connect to nearby HeNB when the macrocell base station, called macro eNB (MeNB), could not provide sufficient service quality. However, the open access policy needs a large number of handovers and signaling between HeNBs and MUEs. This reduces the performance of HeNB. The closed access policy means that only the subscribed HUEs are permitted to access the HeNB. Although it could avoid a large number of handovers and signaling between HeNBs and MUEs, it will generate a severe interference to the nearby MUEs. On the other hand, the hybrid

access policy is the combination of the open access policy and closed access policy. The hybrid access HeNB allows non-subscribed MUEs to use some radio resource to get a basic service. However, the most radio resource of hybrid access HeNB is still allocated to the subscribed HUEs to guarantee their quality-of-service (QoS) requirements.

In the macro-femto system, the channel deployment can be sorted into co-channel deployment, dedicated channel deployment, and partial co-channel deployment [13], [14]. The co-channel deployment means that MeNB and HeNB use the same frequency band to serve their UEs. Although this deployment could enhance the spectral efficiency, it also generates a severe interference between macro and femto networks. On the other hand, the dedicated channel deployment means that MeNB and HeNB use different frequency bands to serve their UEs. The dedicated channel deployment could eliminate the interference to and from macro network. However, it wastes the scare spectrum. As for the partial co-channel deployment, it divides the whole spectrum into two parts. One part is dedicated for MeNB only, and the another part is shared between MeNB and HeNB. The performance of different dividing ratio on the whole spectrum was discussed in [13]. Furthermore, the power control scheme for HeNB can be classified into fixed power scheme and adaptive power scheme. The former indicates that HeNB uses a fixed transmission power to deliver data, and the later indicates that HeNB sets its transmission power according to the variety of the environment.

The HeNB is a user-installed base station. Although the user-installed HeNB is convenient for customers and reduces the cost for operators, the operator cannot know the topology of the randomly deployed HeNBs. This makes that the macrocell system suffers an unexpected interference when MeNB and HeNBs use the same frequency band. Especially when MUE is in the cell-edge region of MeNB, the suffered

interference from HeNBs would make it be out of service. Since there is no connection between MeNB and HeNB, the MeNB cannot inform the HeNB that it generates the interference to MeNB and request it to reduce its transmission power or change its operated frequency.

In order to solve the interference problem and keep the data rate of MUEs under the deployment of co-channel HeNB, Chandrasekhar et al. proposed a utility-based femtocell SINR adaptation scheme by adopting game theory [15]. Here, the utility function is composed of SINR-based reward and penalty, which are related to the interference at the macrocell. Rahman et al. proposed an interference avoidance algorithm in [16], which adopted Hungarian algorithm to design a maximum sum utility. Jo et al. in [17] discussed two interference mitigation strategies for co-channel HeNB to achieve throughput gain. The first strategy adopted the open-loop approach to suppress the cross-tier interference caused by HeNB. The second strategy used the closed-loop approach to satisfy an adaptive interference threshold according to the noise and interference at MeNB. Moreover, in order to avoid the handover of outdoor MUEs, they proposed a coverage coordination scheme for co-channel HeNB based on the measured signal and interference power at HeNB [18]. On the other hand, according to the outage probability of MUEs, Chu et al. proposed a distance-based strategy, which is based on the distance between the closest MeNB, for co-channel HeNB to self-regulate its transmission power and usage of resource [19].

In recent years, cognitive radio (CR) technique is integrated into HeNB to enhance the spectral efficiency of the macro-femto networks [20], [21]. By the definition of Haykin [22], *the cognitive radio is an intelligent wireless communication system that is aware of its surrounding environment (i.e., outside world), and uses the methodology of understanding-by-building to learn from the environment and adapt its internal states to statistical variations in the incoming RF stimuli by making*

corresponding changes in certain operating parameters (e.g., transmit-power, carrier-frequency, and modulation strategy) in real-time, with two primary objectives in mind: highly reliable communications whenever and wherever needed; efficient utilization of the radio spectrum. Thus, the CR-enabled HeNB has the cognitive capability to sense the varying environment, the self-organized capability to analyze and learn from the sensing information, and the reconfigurable capability to use the radio resource flexibly. Therefore, it can adapt to the communication environment and satisfy the network requirements.

There are still some research directions and open issues in the integration of cognitive radio and HeNB [23], such as hardware/firmware modifications, signaling protocol in the femtocell system, inter-working between macro- and femtocell system, business models for open and dynamic access, and the service aspects – authentication, authorization, and accounting (AAA). However, only based on the well-designed resource management scheme and network architecture, operators can achieve the best performance of macro-femto networks more efficiently.

However, the centralized resource management scheme is unrealizable due to the huge number of signaling overhead between MeNB and HeNBs. Therefore, a distributed resource management scheme is suitable for the macro-femto networks. Li et al. proposed a flexible spectrum reuse scheme to solve the interference at femtocell system by adopting the cognitive technique [24]. It was adaptive to the environment by recognizing the *interference signature* from the network, and minimizing the sum of power on the scheduled spectrum. Sahin et al. utilized the scheduling information and spectrum sensing results to decide whether the sub-carriers were occupied so as to reduce both co-channel interference and inter-carrier interference [25]. In [26], da Costa et al. adopted fractional power control [27] as the power control strategy and game-based resource allocation in cognitive environment [28] as the dynamic

spectrum sharing scheme.

Moreover, in order to efficiently execute the radio resource management, the sensing period scheduling was discussed in [29]. Here, the authors studied the QoS-guaranteed sensing period and proposed a resource block allocation scheme. In [30], the strategic game-based resource block management scheme and Gibbs sampler-based resource block management scheme were discussed to mitigate interference among femtocells. Moreover, Cheng et al. analyzed three different resource allocation approaches for CR-enabled HeNB to achieve different levels of spatial reuse [31].

1.2 Thesis Organization

Because there is no connection between MeNB and HeNB, and the available radio resource is insufficient, the interference induced by the closed access HeNBs would degrade performance of its nearby MUEs. Recently, the development of hybrid access femtocell is proposed to solve this problem [32]-[35], and thus HeNB can serve some of its nearby MUEs to offload the traffic of macrocell system, while the hybrid access HeNB has provided service to its HUEs. However, in order to utilize the available radio resource efficiently, and mitigate interfering with neighbor eNBs and UEs, we adopt the cognitive radio technology into our resource management scheme. Also, in order to guarantee the QoS requirements of HUEs, we adopt the priority-based service discipline into our resource management scheme. Therefore, the proposed cognitive priority-based resource management (CPRM) scheme aims to maximize the system throughput of hybrid access HeNB with guaranteeing the QoS requirements of all traffic types.

The remainder of this thesis is organized as follows. Chapter 2 introduces the considered system environment. And, Chapter 3 formulates the resource management

problem of cognitive HeNB in the hybrid access policy, as well as presents the proposed CPRM scheme. Then, the simulation results are provided and analyzed in Chapter 4, and we would conclude our work in Chapter 5.

Chapter 2

System Model

2.1 Macro-Femto Networks

In LTE-A system [36], the macrocell system is a hexagonal grid structure with an MeNB located in the center of coverage, and can be partitioned into three equivalent sectors as illustrated in Figure 2.1. This partition architecture can prevent cell-edge UEs from interference induced by contiguous cell, while we adopt different frequency bands in the three sectors. Since we assume each sector is operated on different frequency bands, and there is the same number of femto blocks randomly overlaid in each sector, we would only focus on one sector of macrocell. Besides, we define the cell-edge region of MeNB as the region where is apart from MeNB by more than four-fifths of its radius.

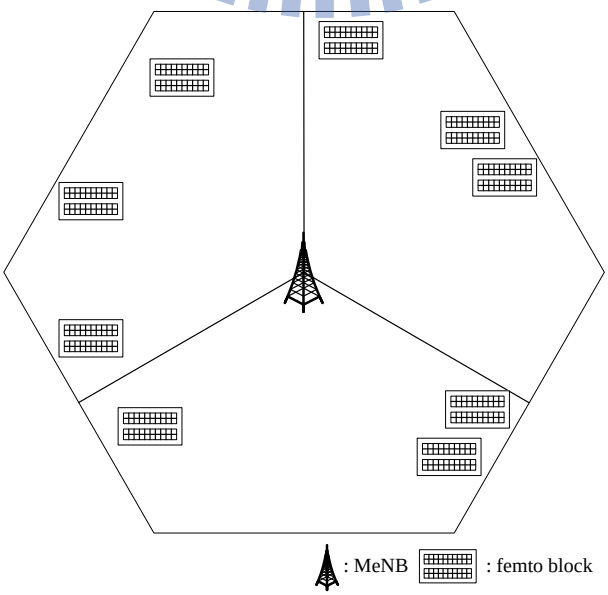

Figure 2.1: Macro-Femto networks.

Furthermore, the femto block is based on dual-strips model and has only one floor for simplicity as shown in Figure 2.2. The femto block consists of 40 apartments, and each apartment can be randomly deployed with one HeNB at most. The deployment ratio of a femto block, denoted by r_d, indicates a ratio of the deployed number of HeNBs over the 40 apartments. As illustrated in Figure 2.2, HUEs are uniformly distributed inside apartments, and MUEs are uniformly distributed outside apartments, while there are a set of Ψ_f HUEs and a set of Ψ_m MUEs in the K serving UEs of hybrid access HeNB.

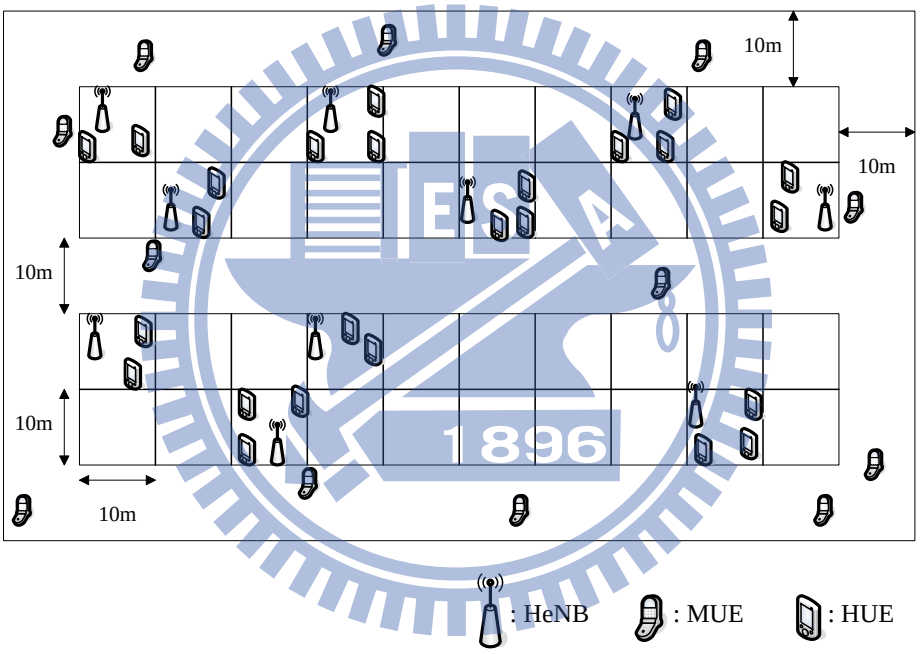

Figure 2.2: Femto block.

Moreover, we consider the frequency division duplexing (FDD) frequency operation mode, and only focus on the downlink transmission bandwidth, denoted by *BW*. The downlink transmission frame structure is shown in Figure 2.3 [37]. Each frame comprises *L* sub-frames, one sub-frame lasts 2 time slots, and there are 7 symbols in a time slot. The *BW* is divided into *N* sub-channels, each sub-channel is grouped by 12 adjacent orthogonal sub-carriers, and each sub-carrier individually spaces 15 kHz. The basic resource unit is sub-frame, and each resource unit contains

N_e allocation units. We assume each sub-channel has flat channel response bandwidth, denoted by BW_{sc}, in a frame duration. Thus, the fading effect coefficients remain constant in each frame, and change from one frame to another one. Under the assumption of the perfect frame synchronization, the cross-talk between frames and inter-symbol interference (ISI) inside frame are neglected. And, the precise OFDM receiver is also supposed to ignore the inter-carrier interference by the property of orthogonality.

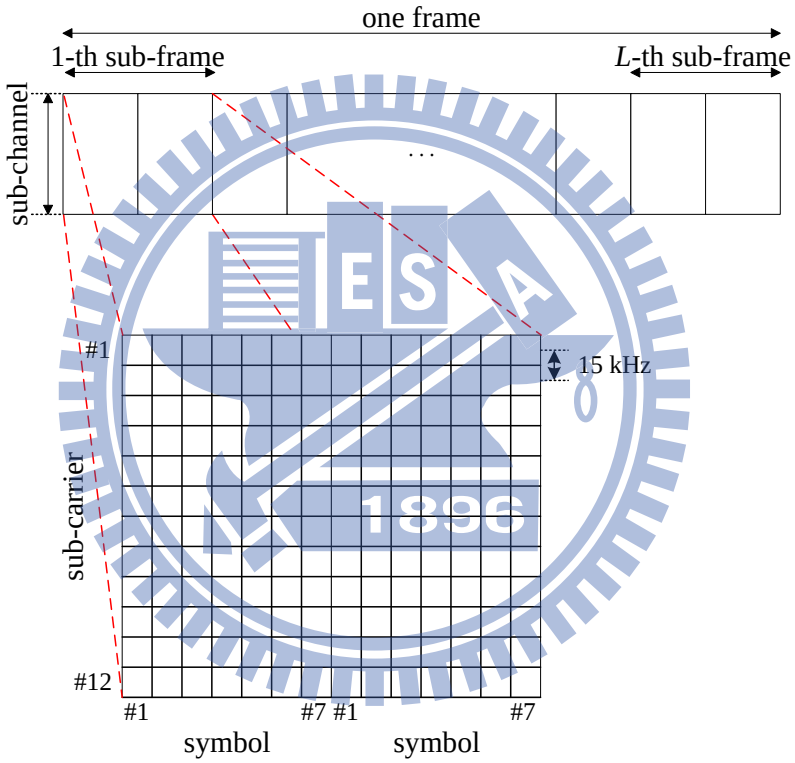

Figure 2.3: Downlink transmission frame structure.

2.2 Channel Model

The wireless fading channel is composed of path-loss, short-term fading, and long-term fading. However, we adopt the path-loss model from [36], and express the path-loss (PL) between receiver R and transmitter T by

$$PL^{R,T} = 10^{-\frac{L_1 + L_2 \log_{10}(d) + L_w}{20}}, \qquad (2.1)$$

where d is the distance in meters between receiver R and transmitter T, L_1= 15.3 and L_2= 37.6 when receiver R is not in the same apartment stripe as transmitter T, L_1= 38.46 and L_2= 20 when receiver R and transmitter T are in the same apartment stripe, and L_w is the penetration loss caused by the walls in the path between receiver R and transmitter T. The short-term fading (JM) between receiver R and transmitter T on the sub-channel n at time t is modeled by Jakes model [38] with M_o oscillators as:

$$JM_n^{R,T} = \sqrt{\frac{2}{M_o}} \times \sum_{m=1}^{M_o} \left\{ \cos\left(2\pi f_D \cos\left(\frac{2\pi m - \pi + \theta}{4M_o}\right)t + \phi \right) + \cos\left(2\pi f_D \sin\left(\frac{2\pi m - \pi + \theta}{4M_o}\right)t + \varphi \right) \right\}, \quad (2.2)$$

where f_D is the Doppler frequency, while θ, ϕ, and φ are statistically independent and uniformly distributed on [-π, π). Moreover, the long-term fading (SF) between receiver R and transmitter T on the sub-channel n is modeled by shadow fading model, which is a log-normal distribution with mean of zero and standard deviation (STD) of σ_{SH} as:

$$SF_n^{R,T} = 10^{-\frac{\sigma_{SH} \times \delta}{20}}, \quad (2.3)$$

where δ is a standard normal distributed variable. Therefore, the channel gain between the receiver R and transmitter T on sub-channel n can be expressed by

$$h_n^{R,T} = PL^{R,T} \times \left| JM_n^{R,T} \right| \times SF_n^{R,T}. \quad (2.4)$$

2.3 Radio Sensing and Power Allocation Mechanism

By CR technique, HeNB would sample the radio environment many times in a sub-frame duration, and the sensed received signal strength (RSS) on sub-channel n is denoted by RSS_n and given by

$$RSS_n = \frac{1}{L_n} \times \sum_{l=1}^{L_n} \sum_{T \in \Omega \setminus F} \left| h_n^{F,T} \right|^2 \times P_{n,l}^T + N_0, \quad (2.5)$$

where L_n is the number of sub-frames required for HeNB to sense sub-channel n, Ω is the set of total eNBs in a sector, $P_{n,l}^{T}$ is the transmitted signal power of transmitter T on the sub-channel n in the l-th sub-frame, and N_0 is the background noise power per sub-channel. Besides, the channel state of sub-channel n, denoted by s_n, is set to be 1 if the signal power on sub-channel n is less than or equal to the threshold of RSS on sub-channel, denoted by RSS_{th}, and 0 otherwise.

HeNB may misjudge the channel state and thus cause false alarm or mis-detection problem. False alarm indicates that HeNB misjudges the available radio resource is unable to use, and mis-detection indicates that HeNB misjudges the unavailable radio resource can be used. Therefore, the probability of false alarm and mis-detection, denoted by P_f and P_m, can be expressed as $P_f = Prob\{RSS_n > RSS_{th} \mid s_n = 1\}$ and $P_m = Prob\{RSS_n \le RSS_{th} \mid s_n = 0\}$.

However, given the sensed RSS_n on sub-channel n and the required SINR for HeNB to transmit b bits to UE k, denoted by $SINR_{k,b}^{*}$, which is given by

$$SINR_{k,b}^{*} = -\frac{\ln(5\times BER_k)}{1.5}\times(2^b - 1), \tag{2.6}$$

where the required BER of UE k is denoted by BER_k, the transmission power of HeNB F on sub-channel n at the l-th sub-frame is determined by

$$P_{n,l}^{F} = SINR_{k,b}^{*}\times\frac{RSS_n}{\left|h_n^{k,F}\right|^2}, \tag{2.7}$$

thus HeNB can transmit bits to its serving UEs and satisfy their BER requirements.

2.4 Traffic Model

Since the storage capacity of eNBs can be enhanced easily by hardware devices, we basically assume that each serving UEs of eNB has infinite buffer. Because multiple services are provided by operators, various service traffics are proposed with

individual characteristics and requirements [39]. We focus on the four most common traffic types, which are voice traffic of real-time (RT) service, video traffic of RT service, HTTP traffic of non-real-time (NRT) service, and FTP traffic of best effort (BE) service.

Although every traffic has the BER requirement, RT service also has the maximum delay tolerance requirement, and NRT service also has the minimum transmission rate requirement. However, the delay of head-of-line (HOL) packet of UE k is denoted by D_k in unit of frames, which is from the arrival of its HOL packet to the current frame, and the maximum delay tolerance of UE k is denoted by D_k^* in unit of frames. Besides, the transmission rate of the UE k to the current frame is denoted by R_k, and its minimum transmission rate is denoted by R_k^*. For RT UE, its packet would be dropped if the packet violates its maximum delay tolerance.

Voice traffic is modeled as a two-state voice activity in Figure 2.4, which corresponds to active and inactive states. The state update is made at the speech encoder periodically with changing probability from active to inactive state of P_a, and that from inactive to active state of P_i. However, it provides different fixed-sized packets to UE in active and inactive states with different fixed periods.

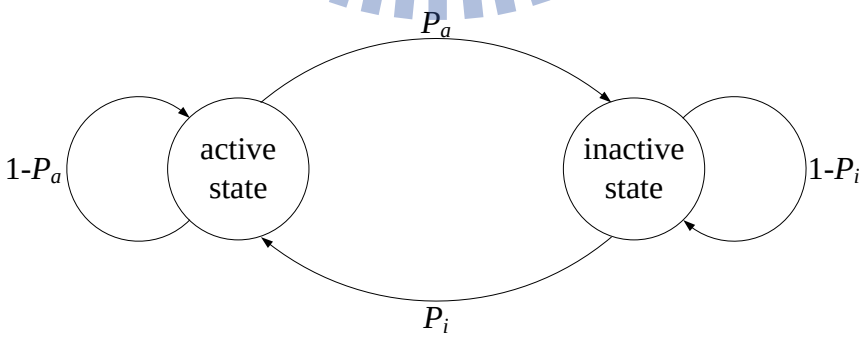

Figure 2.4: Voice traffic model.

Video traffic is modeled as a stable video frame flow in Figure 2.5. It provides a fixed duration and a constant number of packets in one video frame duration.

Moreover, the packet size and the inter-arrival time between packets in a video frame are both based on the truncated Pareto distribution.

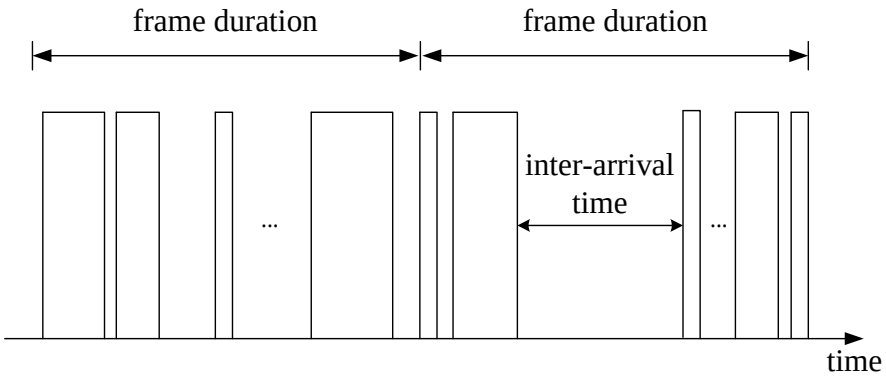

Figure 2.5: Video traffic model.

HTTP traffic is modeled as a web-browsing behavior in Figure 2.6, which includes web-page downloads, reading and parsing duration. The web-page contains a main object and several embedded objects, and the number of embedded objects is based on the truncated Pareto distribution. Besides, the sizes of main and embedded objects are based on the truncated log-normal distribution. The reading duration is the time interval between two web-page downloads, and the parsing duration is the time interval between two objects in a web-page download, while the duration of reading and parsing are both based on the exponential distribution.

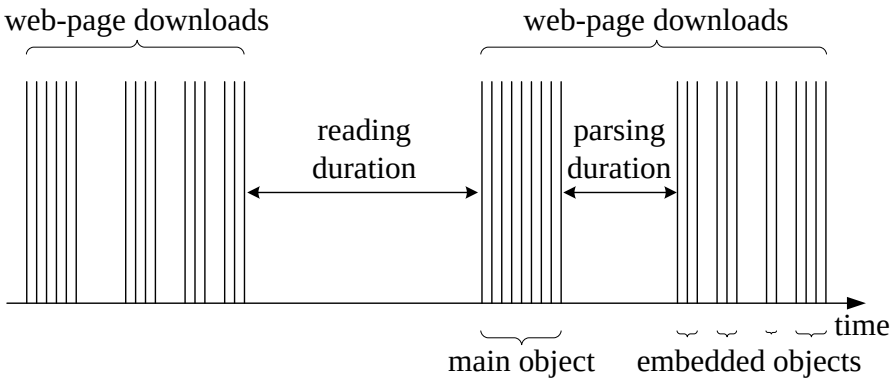

Figure 2.6: HTTP traffic model.

FTP traffic is modeled as a sequence of file downloads in Figure 2.7. Its file size is based on the truncated log-normal distribution, and the inter-arrival time between two successive files is based on the exponential distribution.

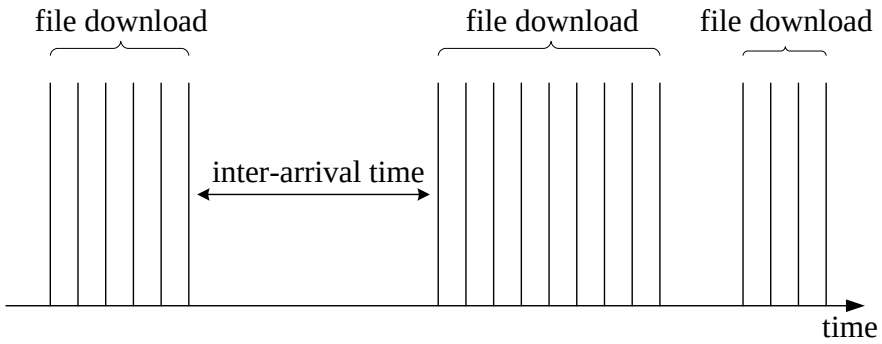

Figure 2.7: FTP traffic model.

However, the detail parameters of each traffic model would be described in Chapter 4.

Chapter 3

Cognitive Priority-based Resource Management Scheme for Macro-Femto Networks

Since the HeNB has the ability of cognitive radio, it could sense all sub-channels and choose the most suitable sub-channels to avoid interfering with MeNB and the neighboring HeNBs. Once the HeNB determines the available sub-channels to transmit data, it allocates sub-channels, modulation order, and power to its serving UEs. Moreover, the HeNB could serve HUEs and MUEs since it adopts the hybrid access policy. Each UE has its QoS requirements, which should be guaranteed by the resource management scheme. Therefore, the problem of radio resource management for the hybrid access HeNB with the ability of cognitive radio is very complex due to its multiple degree of freedom.

In this thesis, we adopt the priority-based service discipline to design a resource management scheme, which determines the priority value to each UE and then serves UEs based on their priority values. In order to maximize the throughput of HeNB and guarantee QoS requirements of its serving UEs, we first formulate the resource management problem of hybrid access HeNB to an optimal problem in the following. After that, we propose a cognitive priority-based resource management (CPRM) scheme to find a sub-optimal solution for this optimal problem.

3.1 Problem Formulation

Define $b_{n,l}^{k}$ as the number of transmission bit on one sub-carrier for UE k with M-QAM modulation on sub-channel n at the l-th sub-frame, where $b_{n,l}^{k} = \log_2 M$ and $b_{n,l}^{k} \in \{0, 2, 4, 6\}$, $1 \le k \le K$, $1 \le n \le N$, and $1 \le l \le L$. If $b_{n,l}^{k} = 0$, it indicates that HeNB does not transmit bits to UE k on sub-channel n at the l-th sub-frame. On the other hand, if $b_{n,l}^{k} = 2$, 4, or 6, it indicates that HeNB transmits data to UE k with the modulation order of QPSK, 16-QAM, or 64-QAM, respectively, on sub-channel n at the l-th sub-frame. Therefore, the total throughput of UE k at the current frame can be obtained by

$$C(\boldsymbol{b}_k) = \sum_{l=1}^{L} \sum_{n=1}^{N} b_{n,l}^{k} \times N_e \times s_n, \quad \forall k, \tag{3.1}$$

where $\boldsymbol{b}_k = \left[b_{1,1}^{k} \cdots b_{1,L}^{k} \cdots b_{1,L}^{k} \cdots b_{n,l}^{k} \cdots b_{n,L}^{k} \cdots b_{N,1}^{k} \cdots b_{N,L}^{k} \right]_{1\times(L\times N)}$.

In the hybrid access HeNB, we should consider the following two QoS fulfillment constraints to guarantee the QoS requirements of UEs and four system constraints to satisfy the limitation of HeNB.

(i) QoS Fulfillment Constraint for RT service

Since the RT UE k has the QoS requirements of the maximum delay tolerance, the delay of its HOL packet, D_k, should be less than or equal to D_k^*. We then have

$$D_k \le D_k^*, \quad \forall k \in \Psi_{RT}, \tag{3.2}$$

where Ψ_{RT} is the set of RT UEs.

(ii) QoS Fulfillment Constraint for NRT service

Since the NRT UE k has the QoS requirements of the minimum transmission rate, its transmission rate, R_k, should be larger than or equal to R_k^*. We then have

$$R_k \geq R_k^*, \quad \forall k \in \Psi_{NRT}, \tag{3.3}$$

where Ψ_{NRT} is the set of NRT UEs. Note that, since BE UE only has the QoS requirement of BER and the BER requirement can be easily fulfilled by setting its transmission power, we do not consider the QoS fulfillment constraint for BE service here.

(iii) Sub-channel Allocation Constraint

In the macro-femto system, a sub-channel can be allocated to at most one UE at each sub-frame, since HeNB is only equipped with one transmit antenna. Thus, the sub-channels allocation constraint is given by

$$\sum_{k=1}^{K} \text{sgn}(b_{n,l}^k) \leq 1, \quad \forall n, l. \tag{3.4}$$

(iv) Power Budget Constraint

The total power allocation for downlink data transmission at HeNB should have a limitation. Let P^* be the maximum transmission power. We then have the power budget constraint as

$$\sum_{n=1}^{N} P_{n,l}^F \leq P^*, \quad \forall l. \tag{3.5}$$

(v) Cognitive Sub-channel Availability Constraint

The sub-channel n is regarded as available if the detected RSS_n is less than or equal to the threshold of RSS, RSS_{th}. Hence, the cognitive sub-channel availability constraint can be expressed by

$$b_{n,l}^k \geq 0, \text{ if } RSS_n \leq RSS_{th}, \quad \forall k, n, l. \tag{3.6}$$

(vi) HUE QoS Satisfaction Constraint

In order to avoid violating the QoS requirements when UE is urgent, each UE should transmit some bits at each frame. Since HeNB is mainly established to serve HUEs, the QoS requirements of HUEs must be guaranteed first. Let γ_k

be the minimum transmission bits of UE k at the current frame. We then have the HUE QoS satisfaction constraint by

$$\sum_{l=1}^{L}\sum_{n=1}^{N} b_{n,l}^{k} \times N_e \geq \gamma_k, \quad \forall k \in \Psi_f. \tag{3.7}$$

Let $\boldsymbol{B} = [\boldsymbol{b_1} \ldots \boldsymbol{b_k} \ldots \boldsymbol{b_K}]$ be the allocation result of HeNB at the current frame. The resource management problem of HeNB can be formulated to an optimal problem as follows,

$$\boldsymbol{B}^* = \arg\max_{\boldsymbol{B}} \sum_{k=1}^{K}\sum_{l=1}^{L}\sum_{n=1}^{N} b_{n,l}^{k} \times N_e \times s_n, \tag{3.8}$$

subject to

QoS fulfillment constraints:

(i) $D_k \leq D_k^*, \quad \forall k \in \Psi_{RT},$

(ii) $R_k \geq R_k^*, \quad \forall k \in \Psi_{NRT},$

and system constraints:

(i) $\sum_{k=1}^{K} \mathrm{sgn}(b_{n,l}^{k}) \leq 1, \quad \forall n, l,$

(ii) $\sum_{n=1}^{N} P_{n,l}^{F} \leq P^*, \quad \forall l,$

(iii) $b_{n,l}^{k} \geq 0, \text{ if } RSS_n \leq RSS_{th}, \quad \forall k, n, l,$

(iv) $\sum_{l=1}^{L}\sum_{n=1}^{N} b_{n,l}^{k} \times N_e \geq \gamma_k, \quad \forall k \in \Psi_f.$

It is complicated to find an optimal solution for the optimal problem of (3.8) by exhaustive search. Therefore, we propose the cognitive priority-based resource management (CPRM) scheme to heuristically find a sub-optimal allocation solution, $\boldsymbol{B}^*$, in (3.8) to maximize the system throughput and satisfy the QoS requirements of UEs.

3.2 Cognitive Priority-based Resource Management Scheme

The cognitive priority-based resource management (CPRM) scheme can sense the available sub-channels from the environment, assign a suitable priority value to each UE, and then allocate the radio resource to UEs according to their priority values. Figure 3.1 shows the HeNB with the CPRM scheme. The CPRM scheme is in charge of sub-channel allocation, modulation assignment, and power allocation for HeNB. It contains three algorithms: cognitive channel determination (CCD) algorithm, priority and minimum bits determination (PBD) algorithm, and priority-based resource allocation (PRA) algorithm.

The input of the CCD algorithm is the sensing information, which is the RSS detected on each sub-channel at the last frame. According to the sensing information, the CCD algorithm determines the number of sub-frames required for HeNB to sense sub-channels and the set of available sub-channels for HeNB. The inputs of the PBD algorithm are users' QoS fulfillment information and queue information. Based on these information, the PBD algorithm assigns a service priority value and the minimum transmission bits to each UE. Note that, the outputs from the CCD and PBD algorithms are the input of the PRA algorithm. The inputs of the PRA algorithm are the channel information, the QoS fulfillment information, the queue information, the set of available sub-channels, UEs' priority values, and their minimum transmission bits. According to these inputs, the PRA algorithm can allocate the suitable sub-channel, modulation order, and transmission power to UEs. Details are given in the following.

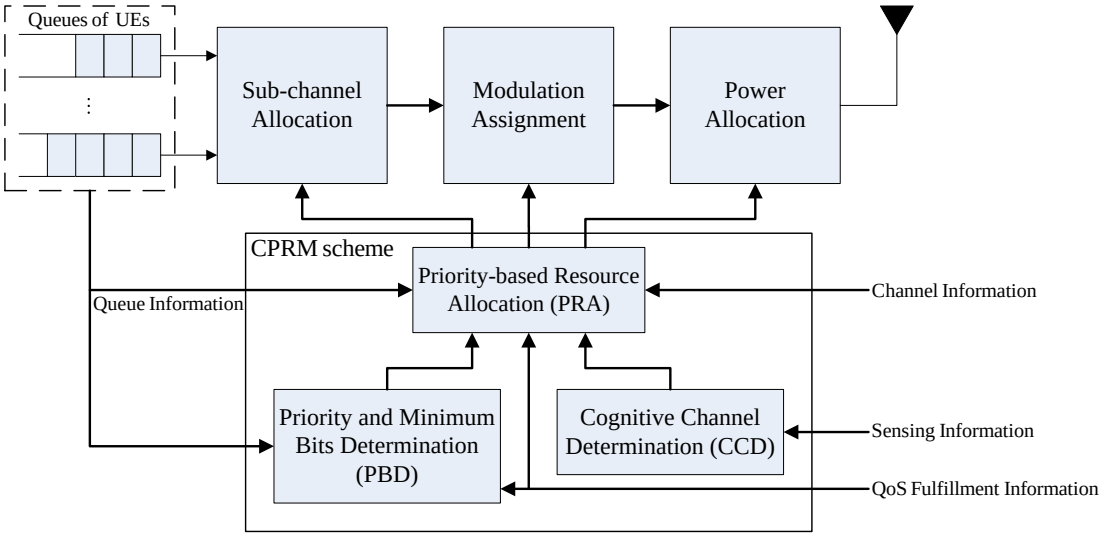

Figure 3.1: The HeNB with the CPRM scheme.

3.2.1 Cognitive Channel Determination Algorithm

The cognitive channel determination (CCD) algorithm determines the minimum number of sub-frames required for HeNB to sense sub-channels, and finds the available sub-channels for HeNB to avoid interfering with MeNB and its neighboring HeNBs. Let L_n be the minimum required number of sub-frames for HeNB to sense sub-channel n, which can be derived by RSS_n, the pre-determined P_f, denoted by P_f^*, and the pre-determined P_m, denoted by P_m^*. Here, the RSS_n is detected at the last frame. The P_f^*, and P_m^* can be expressed by [40], [41]

$$P_f^* = Q\left(\frac{RSS_{th} - N_0}{\sqrt{\frac{2}{L_n \times \chi}} \times \tilde{N}_n}\right) \tag{3.9}$$

and

$$P_m^* = Q\left(\frac{RSS_n - RSS_{th}}{\sqrt{\frac{2}{L_n \times \chi}} \times \tilde{R}_n}\right), \tag{3.10}$$

where χ is the number of sampling for one sensing sub-frame, $\tilde{N}_n$ is the sensing

deviation on sub-channel n in false alarm problem, $\tilde{R}_n$ is the sensing deviation on sub-channel n in mis-detection problem, and $Q(a)$ is the complementary distribution function of the standard Gaussian and is given by

$$Q(a) = \frac{1}{\sqrt{2\pi}} \int_a^{\infty} e^{-\frac{x^2}{2}} dx.$$

We rewrite (3.9) and (3.10) as

$$Q^{-1}(P_f^*) \times \sqrt{\frac{2}{L_n \times \chi}} \times \tilde{N}_n = RSS_{th} - N_0 \tag{3.11}$$

and

$$Q^{-1}(P_m^*) \times \sqrt{\frac{2}{L_n \times \chi}} \times \tilde{R}_n = RSS_n - RSS_{th}, \tag{3.12}$$

respectively. By adding (3.11) and (3.12), we have

$$\sqrt{\frac{2}{L_n \times \chi}} \times \left[Q^{-1}(P_f^*) \times \tilde{N}_n + Q^{-1}(P_m^*) \times \tilde{R}_n \right] = RSS_n - N_0. \tag{3.13}$$

Thus, the L_n can be obtained from (3.13) as

$$L_n = \left\lceil \frac{2 \times (\tilde{N}_n)^2}{(RSS_n - N_0)^2 \chi} \times \left[Q^{-1}(P_f^*) + \frac{\tilde{R}_n}{\tilde{N}_n} \times Q^{-1}(P_m^*) \right]^2 \right\rceil. \tag{3.14}$$

On the other hand, if the sub-channel n satisfies the cognitive sub-channel availability constraint of the system constraint (iii), it would be regarded as the available sub-channel. Therefore, the set of available sub-channels for HeNB, denoted by Φ, is given by

$$\Phi = \left\{ n \middle| RSS_n \le RSS_{th} \text{ and } L_n < L, \forall 1 \le n \le N \right\}. \tag{3.15}$$

3.2.2 Priority and Minimum Bits Determination Algorithm

The priority and minimum bits determination (PBD) algorithm assigns the priority values to UEs according to their packet delay or transmission rate. It also determines the minimum transmission bits at the current frame to UEs based on the

QoS fulfillment information and queue information.

First, we introduce the time-to-expiration (TTE) parameter to represent the degree of urgency of UE [42]. The TTE value for UE k is denoted by V_k in unit of frames and is given by

$$V_k = \begin{cases} D_k^* - D_k, & \text{if } k \in \Psi_{RT}, \\ \left\lfloor \dfrac{B_k + B_k'}{R_k^*} - D_k' \right\rfloor, & \text{if } k \in \Psi_{NRT}, \end{cases} \tag{3.16}$$

where D_k' is the time duration that UE k has buffered HOL packet in the queue, B_k is the number of residual bits of the HOL packet of UE k, and B_k' is the transmitted bits of UE k in D_k'. The smaller the V_k is, the more urgent the UE k is. If $V_k < 0$, it means the UE k violates its QoS requirement. For RT UE k, V_k is derived from its delay requirement. If $V_k \leq 1$, the RT UE k is regarded as urgent, since it will violate its delay requirement and its HOL packet will be dropped after the next frames. On the other hand, for NRT UE k, V_k is derived from its minimum transmission rates; that is $\dfrac{B_k + B_k'}{V_k + D_k'} \geq R_k^*$. If $V_k < 0$, the NRT UE k is regarded as urgent, since it already violates its minimum transmission rate requirement.

We have the following two priority assignment rules:

(i) HUE has a higher service priority than MUE.

(ii) RT UE has a higher priority value than NRT and BE UEs, while urgent NRT UE has a higher priority value than un-urgent RT UE.

Accordingly, the service priority of UE k, denoted by u_k is designed as follows,

$$u_k = \begin{cases} \Delta u_k + \tilde{u}, & \text{if } k \in \Psi_f, \\ \Delta u_k, & \text{if } k \in \Psi_m, \end{cases} \tag{3.17}$$

where Δu_k is the priority value of each service type, and is given by

$$\Delta u_k = \begin{cases} 1+\dfrac{1}{V_k+1}, & \text{if } k \in \Psi_{RT}, \\ \mu, & \text{if } V_k < 0 \text{ and } k \in \Psi_{NRT}, \\ \dfrac{1}{V_k+1}, & \text{if } V_k \geq 0 \text{ and } k \in \Psi_{NRT}, \\ 0, & \text{if } k \in \Psi_{BE}, \end{cases} \tag{3.18}$$

where Ψ_{BE} is the set of BE UEs. In (3.17), HUE k has a higher u_k than MUE by $\tilde{u}$ so as to satisfy the priority assignment rule (i). This can also satisfy the HUE QoS constraint of the system constraint (iv). In this thesis, the value of $\tilde{u}$ is set to be 2.1, because the maximum value of Δu_k is 2. For the same service type, the smaller the V_k is, the larger the Δu_k. The Δu_k of RT UE k is set to be $1+\dfrac{1}{V_k+1}$, which is always larger than that of un-urgent NRT UE, since the maximum value of Δu_k of un-urgent NRT UE k is 1. The Δu_k of urgent NRT UE k is set to be μ, which is between the minimum value of Δu_k for urgent RT UE k (1.5) and the maximum value of Δu_k for un-urgent RT UE k (1.3). Therefore, the priority assignment rule (ii) is satisfied. On the other hand, the Δu_k of BE UE k is set to be 0, since the BE service is the background traffic. By the design of Δu_k, the QoS fulfillment constraints (i) and (ii) can be satisfied.

The minimum number of transmission bits allocated to UE k at the current frame to avoid violating QoS requirements, γ_k, is given as

$$\gamma_k = \begin{cases} \left\lceil \dfrac{B_k}{\max\{1, V_k\}} \right\rceil, & \text{if } k \in \Psi_{RT} \text{ or } \Psi_{NRT}, \\ \min\{3 \times N_e, B_k\}, & \text{if } k \in \Psi_{BE} \text{ and } \Psi_f, \\ 0, & \text{if } k \in \Psi_{BE} \text{ and } \Psi_m. \end{cases} \tag{3.19}$$

For RT or NRT UE k, the value of γ_k is set to be inversely proportional to its TTE value, V_k. If UE k is urgent (V_k = 1 for RT UE and V_k < 1 for NRT UE), its HOL packet should be completely transmitted at the current frame. Because V_k of NRT UE k may be less than 1, the denominator of γ_k is given by $\max\{1, V_k\}$. Since BE HUE is

the subscribed UE of HeNB, it should also get the service. We consider that the BE HUE should obtain at least one resource unit. Thus, the γ_k of BE HUE k is set to be $3\times N_e$, which is the average transmission bits at one resource unit. Moreover, the value of γ_k of BE MUE k is set to be 0, since it is not the subscribed UE of HeNB.

3.2.3 Priority-based Resource Allocation Algorithm

The PRA algorithm allocates sub-channel, modulation order, and transmission power to UEs with the maximum priority value.

Let Ψ_c be the set of backlogged UEs with the maximum priority value, where

$$\Psi_c = \left\{ k \middle| u_k = \max_{1\le k'\le K} u_{k'} \text{ and } B_k > 0,\ \forall 1 \le k \le K \right\}. \tag{3.20}$$

In order to achieve high system throughput and save the transmission power, the optimal pair of UE k^* and sub-channel n^* is selected based on the maximum SINR by

$$(k^*, n^*) = \arg \max_{k\in\Psi_c,\, n\in\Phi} SINR_n^k . \tag{3.21}$$

If there are multiple pairs can achieve the maximum SINR, we randomly select one pair from them. Now, the modulation order is assigned to k^* based on its SINR and power budget constraint. Based on the achievable SINR between UE k^* and HeNB on sub-channel n^*, denoted by $SINR_{n^*}^{k^*}$, $b_{n^*,l}^{k^*}$ is first considered to be set by

$$b_{n^*,l}^{k^*} = \begin{cases} 0, & \text{if } SINR_{n^*}^{k^*} < SINR_{k^*,2}^{*}, \\ 2, & \text{if } SINR_{k^*,2}^{*} \le SINR_{n^*}^{k^*} < SINR_{k^*,4}^{*}, \\ 4, & \text{if } SINR_{k^*,4}^{*} \le SINR_{n^*}^{k^*} < SINR_{k^*,6}^{*}, \\ 6, & \text{if } SINR_{k^*,6}^{*} \le SINR_{n^*}^{k^*}. \end{cases} \tag{3.22}$$

If the required transmission power $P_{n^*,l}^{F}$ satisfies the power budget constraint of the system constraint (ii), the modulation order with $b_{n^*,l}^{k^*}$ is assigned to UE k^*. Otherwise, reduce one modulation order down and check the system constraint (ii) again until

there is no modulation order for this UE. Note that, if $b_{n^*,l}^{k^*} = 0$, it means that there is no suitable sub-channel can be allocated to UE k^*. Thus, UE k^* should be removed from Ψ_c and its priority is set to be -1. The γ_{k^*} is then updated by

$$\gamma_{k^*} = \max\left\{\gamma_{k^*} - b_{n^*,l}^{k^*} \times N_e, 0\right\}. \tag{3.23}$$

Also, the B_{k^*} is updated by

$$B_{k^*} = \max\left\{B_{k^*} - b_{n^*,l}^{k^*} \times N_e, 0\right\}. \tag{3.24}$$

If $\gamma_{k^*} > 0$, the PRA algorithm will allocate the next sub-frame of sub-channel n^* to UE k^* until $\gamma_{k^*} = 0$ or the sub-channel n^* has no void sub-frame.

Once the resource allocated to UE k^* is completed, the CPRM scheme sets its priority value to be 0 and looks for another best pair of (k^*, n^*). If the sub-channel n^* has no void sub-frame for data transmission, it is removed from Φ. Note that, in order to satisfy the sub-channel allocation constraint of the system constraint (i), one sub-channel is allocated to one UE at each sub-frame. If there is still the residual resource after all UEs are served ($u_k \le 0$, $1 \le k \le K$), the PRA algorithm sets $\gamma_k = B_k$, $1 \le k \le K$, and redo (3.21) to allocate the residual resource to the backlogged UE with the maximum SINR. The procedure of the PRA algorithm is repeated until all radio resource is allocated to the selected UEs or no backlogged UEs exists.

3.2.4 Summary of The CPRM Scheme

Based on the CCD, PBD, and PRA algorithms, the CPRM scheme can find a sub-optimal solution for (3.8) to maximize the system throughput of HeNB, and guarantees the QoS requirements of its serving UEs. The CPRM scheme can be summarized as the following five steps.

Step 1. Initialize the CPRM scheme. Set L_n of all sub-channels by (3.14) in the CCD algorithm. Also, set u_k and γ_k of all serving UEs by (3.17) and (3.19),

respectively, in the PBD algorithm.

Step 2. Find the set of the available sub-channels, Φ, by (3.15) in the CCD algorithm. Only when $|\Phi| > 0$ and $l \le L$, the CPRM scheme would go to step 3.

Step 3. Find a pair of UE k^* and sub-channel n^* by (3.21) in the PRA algorithm. Then, allocate suitable $b_{n^*,l}^{k^*}$ and $P_{n^*,l}^{F}$ by (3.22) and (2.7), respectively, to UE k^* on sub-channel n^* at the l-th sub-frame. If $|\Psi_c| = 0$, end.

Step 4. Pre-allocate the next sub-frame to the selected UE k^*. If $\gamma_{k^*} > 0$ and $l' \le L$, set $b_{n^*,l'}^{k^*} = b_{n^*,l}^{k^*}$, and $P_{n^*,l'}^{F}$ by (2.7), $l+1 \le l' \le L$, until $\gamma_{k^*} = 0$.

Step 5. If $|\Phi| > 0$ and $\gamma_{k^*} > 0$, go to step 3. If $|\Phi| > 0$ and $u_k \le 0$, $1 \le k \le K$, set $\gamma_k = B_k$, $1 \le k \le K$, and go to step 3. If $|\Phi| = 0$, end.

The pseudo code of the CPRM scheme is given as follows.

Input : $h_n^{k,F}$, $\forall 1 \le k \le K$, $1 \le n \le N$, RSS_n, $\forall 1 \le n \le N$, and D_k^*, R_k^*, D_k, R_k, D_k', B_k, B_k', BER_k, $\forall 1 \le k \le K$.
Output : $b_{n,l}^k$, $\forall 1 \le k \le K$, $1 \le n \le N$, $L_n < l \le L$.

1: // Initialize the CPRM scheme.
2: Set L_n by (3.14), u_k by (3.17), and γ_k by (3.19).
3: // Find the set of available sub-channels.
4: Find Φ by (3.15).
5: // If there is available sub-channel, perform the CPRM scheme.
6: **while** $|\Phi| > 0$ and $l \le L$ **then**
7: Set Ψ_c by (3.20).
8: // If no candidate UE,end.
9: **if** $|\Psi_c| == 0$ **then**
10: **break**
11: **end if**
12: // Find an optimal pair of UE and sub-channel.
13: Find (k^*, n^*) by (3.21).
14: // Allocate bits and power to UE k^* on sub-channel n^*.
15: Set $b_{n^*,l}^{k^*}$ by (3.22), and $P_{n^*,l}^{F}$ by (2.7).
16: // Check the system constraint (ii).
17: **while** $\sum_{n=1}^{N} P_{n,l}^{F} > P^*$ **then**
18: Set $b_{n^*,l}^{k^*} = b_{n^*,l}^{k^*} - 2$, and $P_{n^*,l}^{F}$ by (2.7).
19: **end while**
20: // If no suitable modulation order to UE k^*, remove it from Ψ_c.
21: **if** $b_{n^*,l}^{k^*} == 0$ **then**
22: Set $\Psi_c = \Psi_c - \{k^*\}$, u_{k^*} = -1.
23: Go to line 7.
24: **end if**

25: Update γ_{k^*} by (3.23) and B_{k^*} by (3.24).
26: Set $l' = l + 1$.
27: // Pre-allocate resource to UE k^* on sub-channel n^*.
28: **while** $\gamma_{k^*} > 0$ and $l' \le L$ **then**
29: Set $b^{k^*}_{n^*,l'} = b^{k^*}_{n^*,l}$, $P^F_{n^*,l'}$ by (2.7), and $l' = l' + 1$.
30: Update γ_{k^*} by (3.23) and B_{k^*} by (3.24).
31: **end while**
32: Update u_{k^*} and Φ
33: // If there is residual resource and UE k^* still has the required bits, continue to allocate the resource to the UE with the required bits.
34: **if** $|\Phi| > 0$ and $\gamma_{k^*} > 0$ **then**
35: Go to line 7.
36: // If there is residual resource and all backlogged UEs can compete it, allocate the resource to the UE with their residual HOL packet bits.
37: **elseif** $|\Phi| > 0$ and $u_k \le 0$, $\forall 1 \le k \le K$, **then**
38: Set $\gamma_k = B_k$, $\forall 1 \le k \le K$.
39: Go to line 7.
40: **end if**
41: **end while**

Chapter 4

Simulation Results

4.1 Simulation Environment

In the simulations, parameters of the considered macro-femto networks are set to be compatible with the 3GPP E-UTRA standard [36]. The parameter values are listed in Table 4.1. The system bandwidth in each sector is 5 MHz, which is divided into 25 sub-channels. Each sub-channel has 144 allocation units for data transmission. Therefore, the maximum transmission rate per macro sector is equal to 21.6 Mbps, which is obtained when each sub-channel delivers data by the highest modulation order of 64-QAM. Each sector has 3 femto blocks with the same number of deployed HeNBs of 16. The total traffic intensity (ρ) is defined as

$$\rho = \frac{\text{total arrival rates of all traffics}}{\text{maximum transmission rate per macro sector}}. \quad (4.1)$$

In each femto block, the numbers of voice, video, HTTP, and FTP UEs are set to be the same, and each HeNB is deployed with the same number of HUEs. The number of MUE is twice than that of HUE in each traffic type. Each HUE would stay in a fixed position, and each MUE would move in any direction from [-π, π) with constant speed of 3 km/hr. If total resource units in a frame duration are equally divided to HeNBs in a femto block without overlapping, then we assume every HeNB would utilize at most 15 resource units for data transmission in a frame duration. Besides, we assume that MeNB has utilized total bandwidth, and divides its total

transmission power fairly on the bandwidth. On the other hand, if MUE that needs service can detect the highest average SINR on bandwidth among HeNBs whose serving UE number is less than the maximum number of serving UEs, we assume the MUE would automatically hand over to that HeNB in the beginning of frame.

However, to evaluate the throughput gain from the deployment of HeNBs, we will consider the pure macro network. The pure macro network is similar to the macro-femto networks but only one difference, which is that all HeNBs are disabled and MeNB would use total bandwidth to serve all HUEs and MUEs.

Table 4.1: Parameters of the macro-femto networks.

Parameters	**Value**
Carrier frequency	2 GHz
Frame duration	10 ms
Number of sub-frames in a frame duration (L)	10
Radius of macrocell	1000 m
Radius of femtocell	10 m
Total transmission power of MeNB	43 dBm
Total transmission power of HeNB (P^*)	20 dBm
Pre-determined probability of false-alarm (P_f^*)	0.1
Pre-determined probability of mis-detection (P_m^*)	0.1
Thermal noise density	-174 dBm/Hz

4.2 Traffic Model and QoS Requirements

Since the voice traffic is modeled as a two-state voice activity, the state update is made at the speech encoder every 20 ms with changing probability from active to inactive state of 0.1, and that from inactive to active state of 0.1. During the active period, the encoder generates a 40 bytes packet to UE every 20 ms. During the inactive period, the encoder generates a 15 bytes packet to UE every 160 ms. Thus, the arrival rate of voice traffic is 8.375 Kbps.

In the video traffic, the video frame arrives every 100 ms, and contains 8 packets,

while the size of packet and the inter-arrival time between packets are both truncated Pareto distributed. The parameters of the size of packet and the inter-arrival time are given in Table 4.2, and the arrival rate of video traffic is 64 Kbps.

Table 4.2: Video traffic model parameters.

Component	**Distribution**	**Parameters**
Packet size	Truncated Pareto	Min. = 40 bytes, Max. = 250 bytes, Mean = 100 bytes, $\alpha = 1.2$
Inter-arrival time between packets in a frame	Truncated Pareto	Min. = 2.5 ms, Max. = 12.5 ms, Mean = 6 ms, $\alpha = 1.2$

In the HTTP traffic, the reading duration and the parsing duration are exponential distributed with mean of 30 s and 0.13 s, respectively. The sizes of main and embedded objects are truncated log-normal distributed. The number of embedded objects is truncated Pareto distributed. The parameters of the sizes of main and embedded objects, as well as the number of embedded objects are given in Table 4.3, and the arrival rate of HTTP traffic is 14.178 Kbps.

Table 4.3: HTTP traffic model parameters.

Component	**Distribution**	**Parameters**
Main object size	Truncated Log-normal	Min. = 100 bytes, Max. = 2 Mbytes, Mean = 10710 bytes, std. dev. = 25032 bytes
Embedded object size	Truncated Log-normal	Min. = 50 bytes, Max. = 2 Mbytes, Mean = 7758 bytes, std. dev. = 126168 bytes
Number of embedded objects per page	Truncated Pareto	Max. = 53, Mean = 5.64

In the FTP traffic, the FTP file size is truncated log-normal distributed, and the inter-arrival time between two successive files is exponential distributed with mean of 180 s. The parameters of the file size are given in Table 4.4, and the arrival rate of FTP traffic is 88.89 Kbps.

Table 4.4: FTP traffic model parameters.

Component	**Distribution**	**Parameters**
File size	Truncated Log-normal	Min. = 50 bytes, Max. = 5 Mbytes, Mean = 2 Mbytes, std. dev. = 722 Kbytes

Moreover, the QoS requirements of each traffic type are listed in Table 4.5.

Table 4.5: QoS requirements of each traffic type.

Traffic type / **Requirement**	**Voice**	**Video**	**HTTP**	**FTP**
Required BER	10^{-3}	10^{-4}	10^{-6}	10^{-6}
Max. packet delay tolerance	40 ms	100 ms	N/A	N/A
Max. allowable dropping rate	1%	1%	N/A	N/A
Min. required transmission rate	N/A	N/A	100 Kbps	N/A

N/A: Not Applicable

4.3 Conventional Schemes

In the simulations, we would compare the proposed CPRM scheme with two conventional schemes, which are decomposion-based resource management (DBRM) scheme [43] and cognitive radio resource management (CRRM) scheme [44]. Both the DBRM and CRRM schemes are representative schemes for cognitive femtocell, and the details of these two schemes are given in the following.

4.3.1 Decomposition-based Resource Management Scheme

The HeNB would sense one sub-frame to indicate the set of available sub-channels in the beginning of frame, and then performs the DBRM scheme. The DBRM scheme aims to maximize the throughput of HeNB by employing the decomposition methods. It decomposes the resource allocation problem into master problem for channel allocation, and sub-problem for power allocation. The channel allocation on sub-channel c of HeNB i to UE j is based on the g_{ijc}, which is defined as

$$g_{ijc} = \frac{h_{ijc}}{I_{ijc} + N_0}, \tag{4.2}$$

where h_{ijc} (I_{ijc}) is the channel gain (sensed interference) between HeNB i to UE j on sub-channel c. HeNB i would allocate an available sub-channel c^* to UE j^*, if $g_{ij^*c^*}$ has the maximum value. Then, remove sub-channel c^* and UE j^* from its set of available sub-channels and UEs, and then repeat the channel and UE allocation until there is no sub-channel or UE left.

Based on the channel allocation result, HeNB i would determine the transmission power to UE j on sub- channel c by

$$P_{ijc} = \left[\frac{1}{K} P^* + \frac{1}{K} \sum_{1 \le k \le K} \frac{1}{g_{ikc_k}} - \frac{1}{g_{ijc}} \right]_{\tilde{P}_{ijc}}^{P^*}, \tag{4.3}$$

where c_k is the allocated channel to UE k, and $\tilde{P}_{ijc}$ is the minimum required power for HeNB i to achieve the minimum required SINR for UE j on sub-channel c. Because the DBRM scheme only consider the channel condition between HeNB and UE, it would treat HUE and MUE in the same manner. Furthermore, there are four traffic types in the network, and each traffic type has different QoS requirements. To make a fair comparison, we would allocate resource to urgent UE first in the DBRM scheme so as to guarantee the QoS requirements of UEs.

4.3.2 Cognitive Radio Resource Management Scheme

In the beginning of sensing period, denoted by T_s, HeNB would sense one sub-frame duration to indicate the set of available sub-channels, and then performs the CRRM scheme. The CRRM scheme aims to achieve fully radio resource utilization and guarantee the QoS requirements of RT UEs statistically by deriving the effective capacity. We set the QoS exponent by the arrival rate of voice traffic for stringent QoS requirement. Besides, we set both the resource allocation correlation probability of MeNB and the percentage of correlated resource to present the high correlated allocation of MeNB as in [44].

Based on the derived effective capacity and the sensed information, which is the percentage of un-available resource, HeNB would find T_s and the required minimum number of resource unit to satisfy the delay requirements of RT UEs. Then, HeNB would randomly allocate the required minimum number of resource units to its serving UEs from the available radio resource regardless of the channel condition and the kind of serving UE. Hence, the CRRM scheme would also treat HUE and MUE in the same manner.

In order to accept the service request of MUE accurately in the beginning of frame, and make a fair comparison, we would fix T_s by one frame duration. However, there is NRT UE in the network, and the NRT UE also has the QoS requirement of the minimum transmission rate. To make a fair comparison, we would also find the required minimum number of resource to satisfy the minimum transmission rate requirement of NRT UE statistically, and then allocate resource to urgent UE first to satisfy the QoS requirement of UE in the CRRM scheme. Besides, since there is no power allocation scheme proposed in the CRRM scheme, we would allocate power by (2.7) to satisfy the BER requirement of UE.

4.4 System Parameters Adjustment

To observe the throughput gain from the deployment of HeNBs in the cell-edge region, we observe throughput of MeNB in the pure macro network and that of HeNBs in the macro-femto networks. In the pure macro network, there is no other deployed eNBs, and then MeNB could use the total bandwidth without interfered by other eNBs. Moreover, HUEs and MUEs are sub-scribed to MeNB, while HUEs are still deployed inside the apartment, and MUEs are deployed outside the apartment. In this scenario, MeNB only performs the PBD and PRA algorithms, and the biased priority value for HUE, $\tilde{u}$, is set to be 0.

Figure 4.1 shows the throughput of UEs, throughput of HUEs, and throughput of MUEs in the macro-femto and pure macro networks. It can be observed that the throughput of UEs, throughput of HUEs, and throughput of MUEs in the macro-femto networks are larger by more than 47.5%, 54.4%, and 43.9%, compared to those in the pure macro network, as the total traffic intensity is larger than 0.58. Besides, HUEs have throughput degradation of 13.2%, and MUEs have throughput increase of 24.2%, when the total traffic intensity is larger than 1.17. The first phenomenon is due to the fact that the cell-edge UEs have bad channel condition, and MeNB cannot transmit data to them with high modulation order. The second phenomenon is because HUEs usually have worse channel condition than MUEs, and there is insufficient resource to serve all UEs as the total traffic intensity increases. Then, MeNB would tend to serve MUEs prior to HUEs.

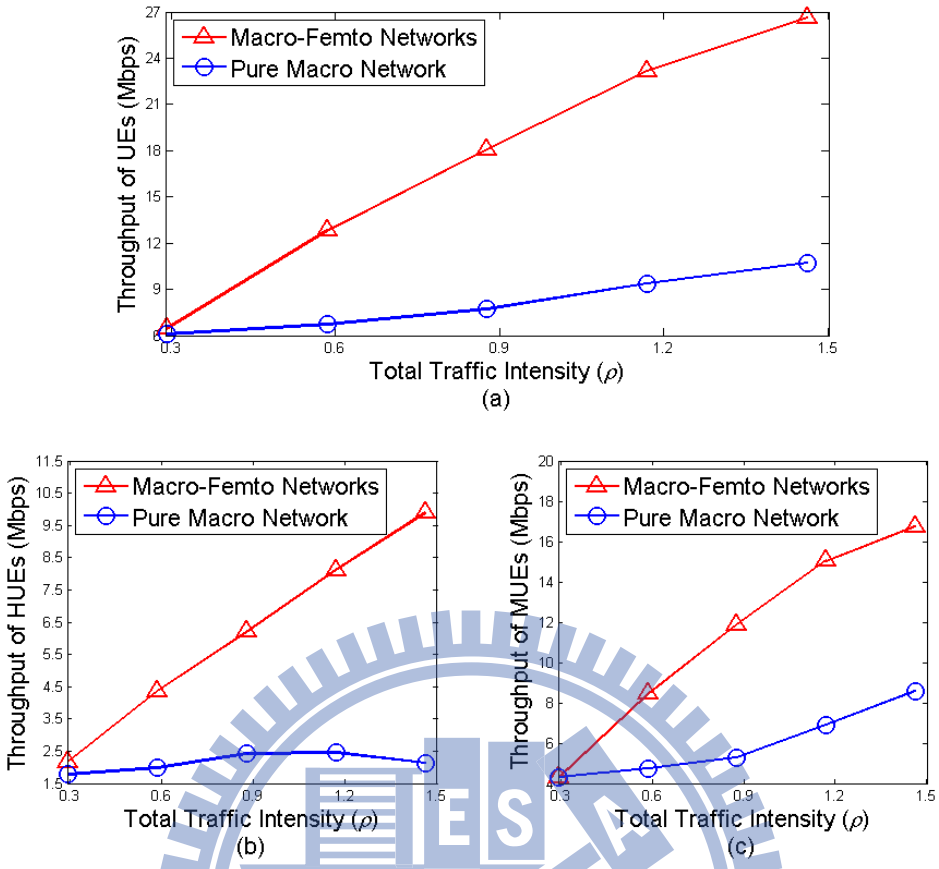

Figure 4.1 (a) Throughput of UEs, (b) throughput of HUEs, and (c) throughput of MUEs in the macro-femto and pure macro networks.

Since the number of serving UEs of hybrid access HeNB is limited by the K_{max}, and thus MUEs could establish connection to hybrid access HeNB, when the number of serving UEs of hybrid access HeNB is smaller than the K_{max}. Moreover, different values of K_{max} would affect the performance of the CPRM scheme, and thus we would observe the performance of the CPRM scheme in K_{max} of 10, 15, and 20.

Figure 4.2 illustrates the throughput of UEs, throughput of HUEs, and throughput of MUEs. In the total traffic intensity of 1.46, we can find that the throughput of UEs, throughput of HUEs, and throughput of MUEs in K_{max} of 15 are slightly smaller by 0.9%, 1.4%, and 0.7%, compared to those in K_{max} of 10. Besides, throughput of HUEs is similar in K_{max} of 15 and 20, while throughput of UEs and throughput of MUEs in K_{max} of 15 are slightly larger by 0.5% and 0.8%, compared to those in K_{max} of 20. This consequence is because the CPRM scheme tends to serve the urgent UEs

first to satisfy the QoS requirements, and then serve the UEs with better channel condition to maximize the throughput of UEs, while the CPRM scheme in smaller K_{max} would have less urgent UEs.

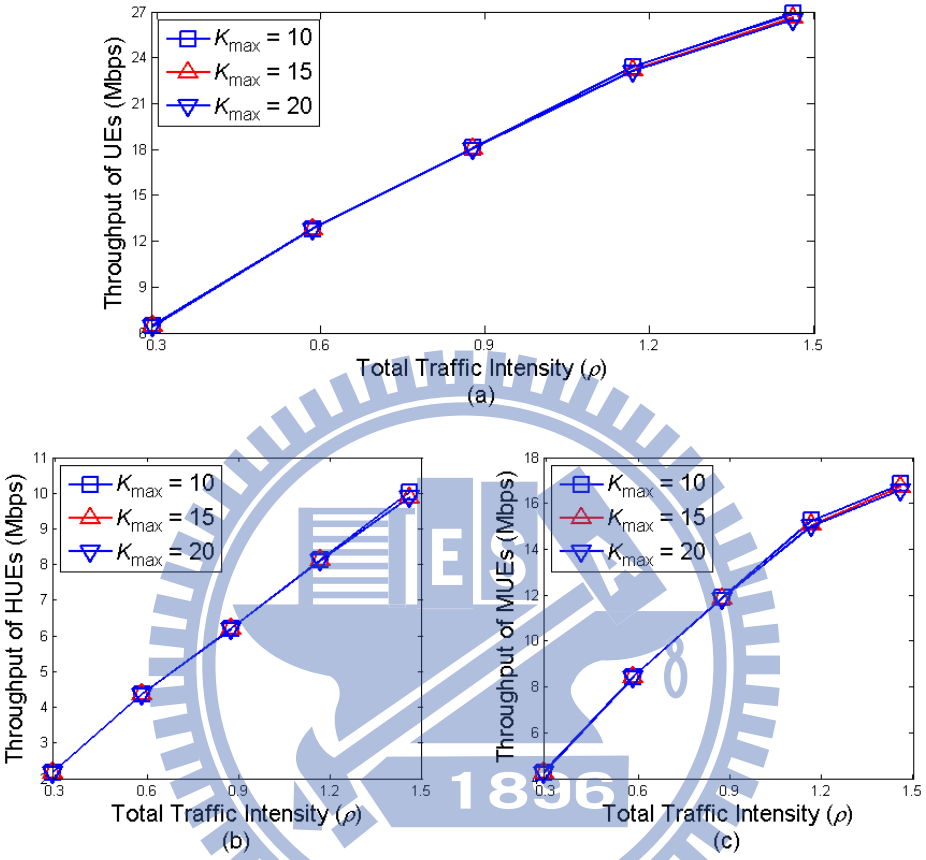

Figure 4.2 (a) Throughput of UEs, (b) throughput of HUEs, and (c) throughput of MUEs.

Figure 4.3 presents the packet dropping rate of voice and video UEs, while Figure 4.4 presents the packet dropping rate of voice HUEs and MUEs, as well as that of video HUEs and MUEs. It can be seen that the packet dropping rate of voice and video UEs in K_{max} of 10 is smaller than that in K_{max} of 15, while the packet dropping rate of voice and video UEs in K_{max} of 20 violates the packet dropping rate requirement in the total traffic intensity of 1.46. Besides, the packet dropping rate of video UEs in K_{max} of 10 increases rapidly as the total traffic intensity increases. The first phenomenon is due to the fact that there would be less urgent UEs in smaller

K_{max}, and the CPRM scheme in smaller K_{max} would have more resource to guarantee the delay tolerance requirements of voice and video UEs. However, the CPRM scheme in K_{max} of 20 accepts too many voice and video MUEs, and has insufficient resource to guarantee their delay tolerance requirements. However, the second phenomenon is because the video packet size is large, and the video MUEs might be served by HeNB that cannot transmit data with high modulation order. Furthermore, those HeNB might be unable to provide the basic service to video MUEs as the total traffic intensity increases

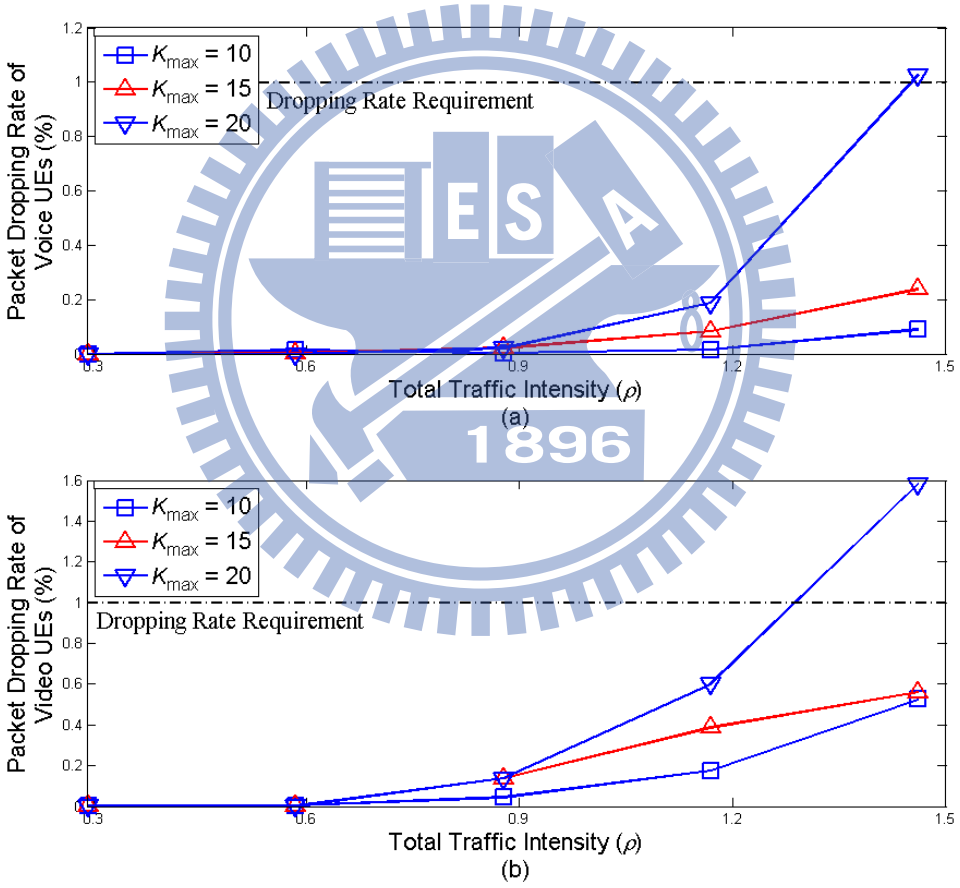

Figure 4.3 Packet dropping rate of (a) voice and (b) video UEs.

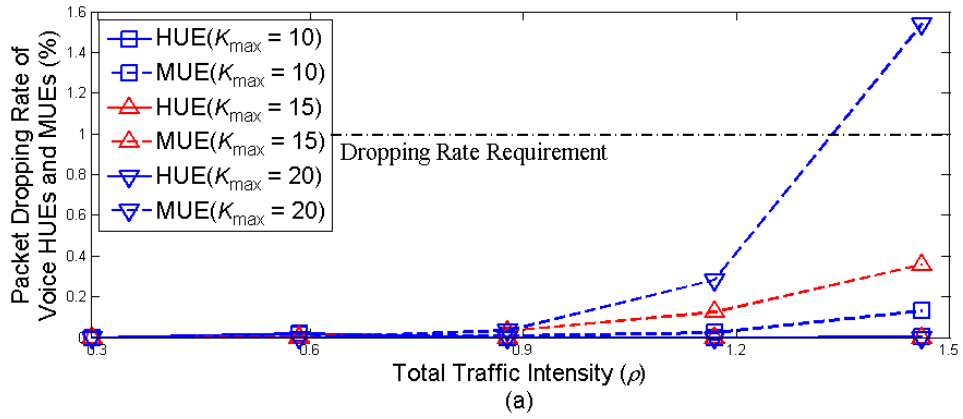

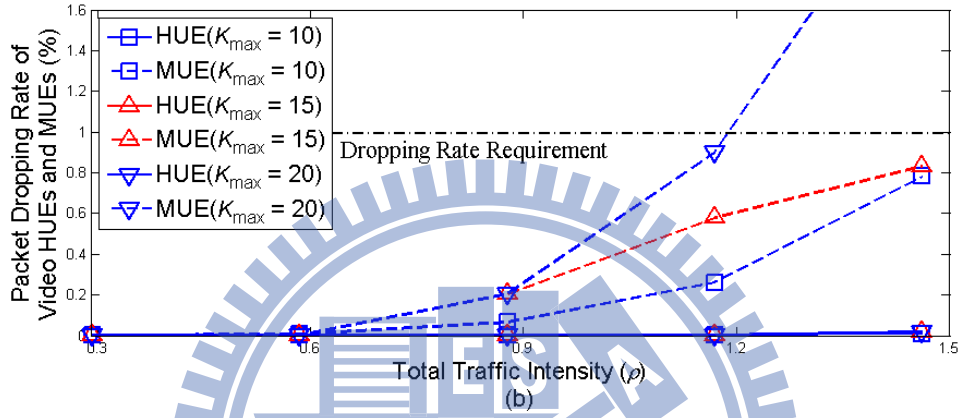

Figure 4.4 Packet dropping rate of (a) voice HUEs and MUEs, as well as (b) video HUEs and MUEs.

However, since the throughput of UEs in K_{max} of 15 is similar to that K_{max} of 10, and the CPRM scheme in K_{max} of 15 can satisfy the QoS requirements of all traffic types, as well as it does not have rapid increasing packet dropping rate of video MUEs, we set K_{max} to be 15 and evaluate the performance. Besides, we would adjust the deployment ratio of femto block, r_d, and then evaluate the performance.

Figure 4.5 exhibits the throughput of UEs, throughput of HUEs, and throughput of MUEs. It can be learned that the CPRM scheme in r_d of 0.2 has the smallest throughput of UEs, throughput of HUEs, and throughput of MUEs. Besides, it has dramatic decreasing throughput of MUEs as the total traffic intensity exceeds 0.88. However, the CPRM scheme in r_d of 0.6 has larger throughput of UEs, throughput of HUEs, and throughput of MUEs, compared to those of the CPRM scheme in r_d of 0.4, after the total traffic intensity is 0.88. The first consequence is because there are less

HeNBs in smaller r_d, and thus less UEs would be served. Moreover, the second consequence is also because there are too many UEs for HeNBs to serve in r_d of 0.2, and then MUEs have dramatic decreasing throughput. On the other hand, the third consequence is due to the fact that there are more HeNBs in r_d of 0.6, and thus more interference would be generated. Therefore, the CPRM scheme in r_d of 0.4 can achieve larger throughput to UEs than the CPRM scheme in r_d of 0.6, before it can only achieve similar throughput of HUEs to the CPRM scheme in r_d of 0.6, but smaller throughput of MUEs than the CPRM scheme in r_d of 0.6.

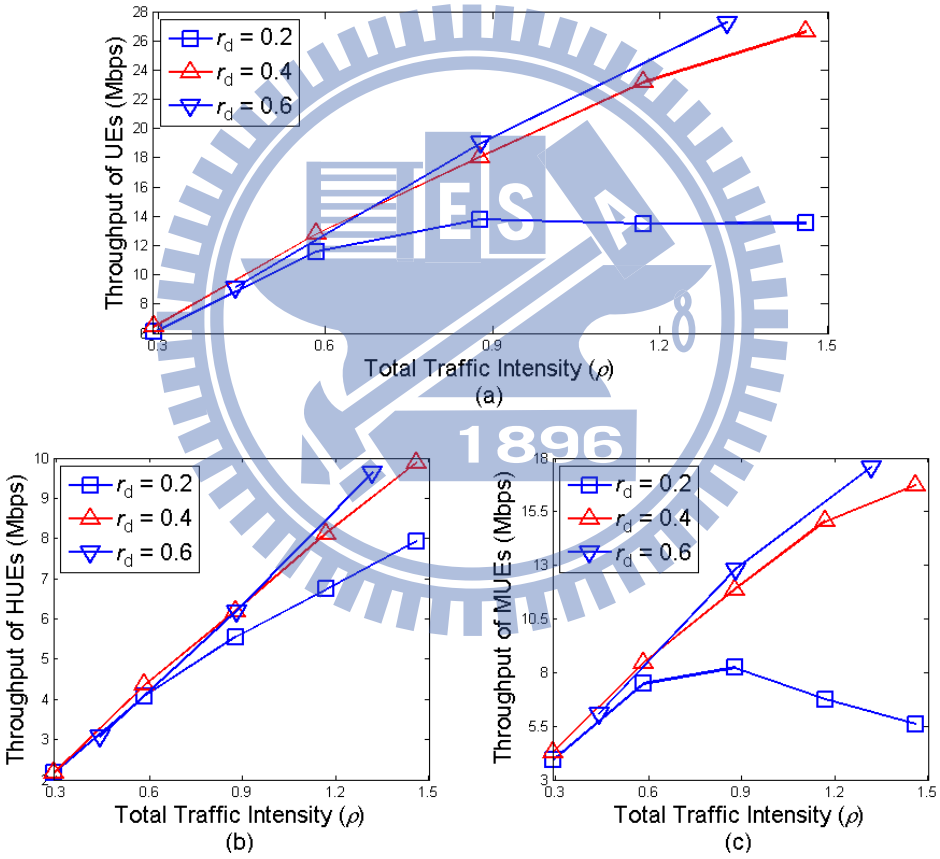

Figure 4.5 (a) Throughput of UEs, (b) throughput of HUEs, and (c) throughput of MUEs.

Figure 4.6 depicts the packet dropping rate of voice and video UEs, while Figure 4.7 depicts the packet dropping rate of voice HUEs and MUEs, as well as that of video HUEs and MUEs. We can notice that the CPRM scheme in r_d of 0.2 violates the

packet dropping rate of voice and video UEs and that of MUEs in the total traffic intensity of 0.88. Besides, the CPRM scheme in r_d of 0.6 has smaller packet dropping rate of voice and video UEs, compared to that of the CPRM scheme in r_d of 0.4. The first phenomenon is because there are not enough HeNBs to serve the MUEs in smaller r_d, and then voice and video MUEs have dramatic increasing packet dropping rate as the total traffic intensity increases. Moreover, the second phenomenon is due to that there are more HeNBs in larger r_d, and thus more MUEs could be served.

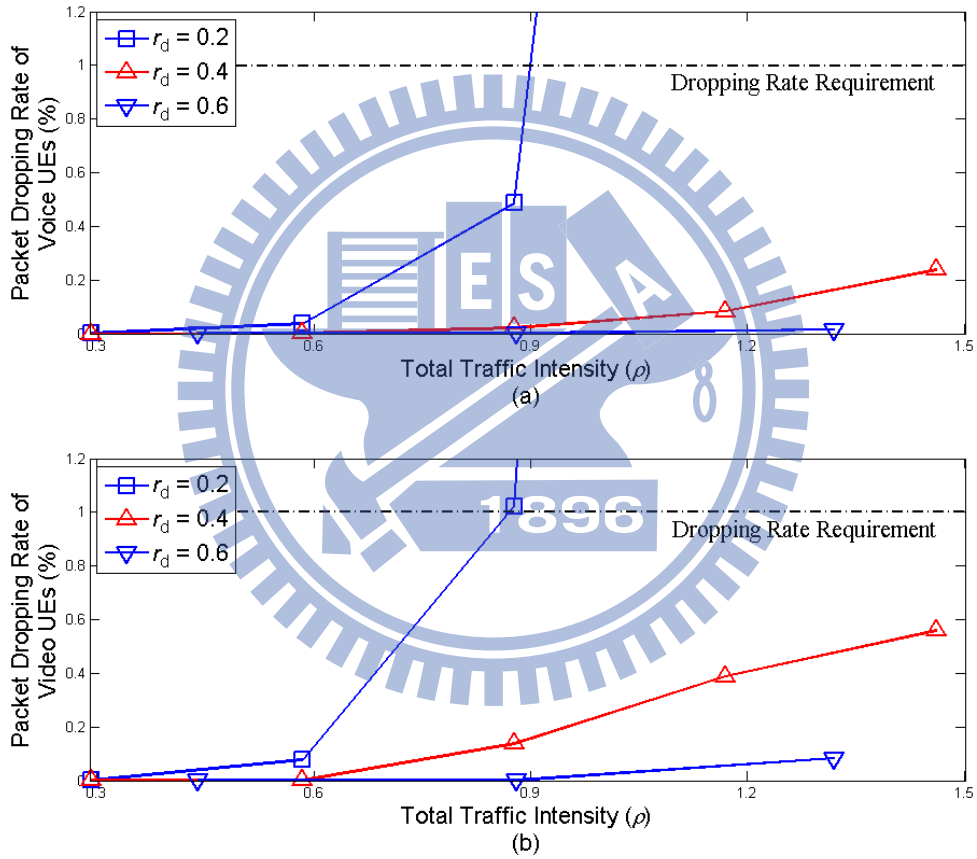

Figure 4.6 Packet dropping rate of (a) voice and (b) video UEs.

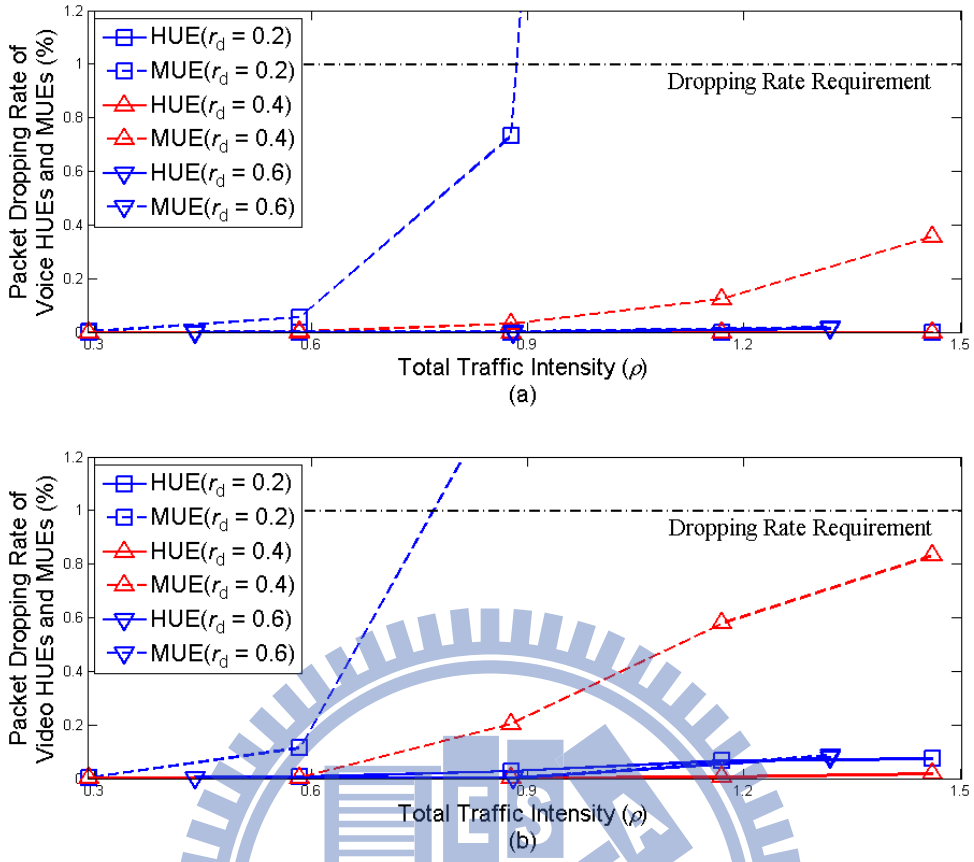

Figure 4.7 Packet dropping rate of (a) voice HUEs and MUEs, as well as (b) video HUEs and MUEs.

Figure 4.8 shows the average transmission rate of HTTP UEs, as well as that of HTTP HUEs and MUEs. We can discover that the CPRM scheme in r_d of 0.2 would violate the minimum transmission rate of HTTP UEs as the total traffic intensity is larger than 0.88, and violates that of HTTP HUEs and MUEs in the total traffic intensity of 0.88 and 1.17, respectively. Furthermore, the CPRM scheme in r_d of 0.6 can achieve the largest transmission rate of HTTP UEs. These consequences can be explained as in Figure 4.6 and 4.7.

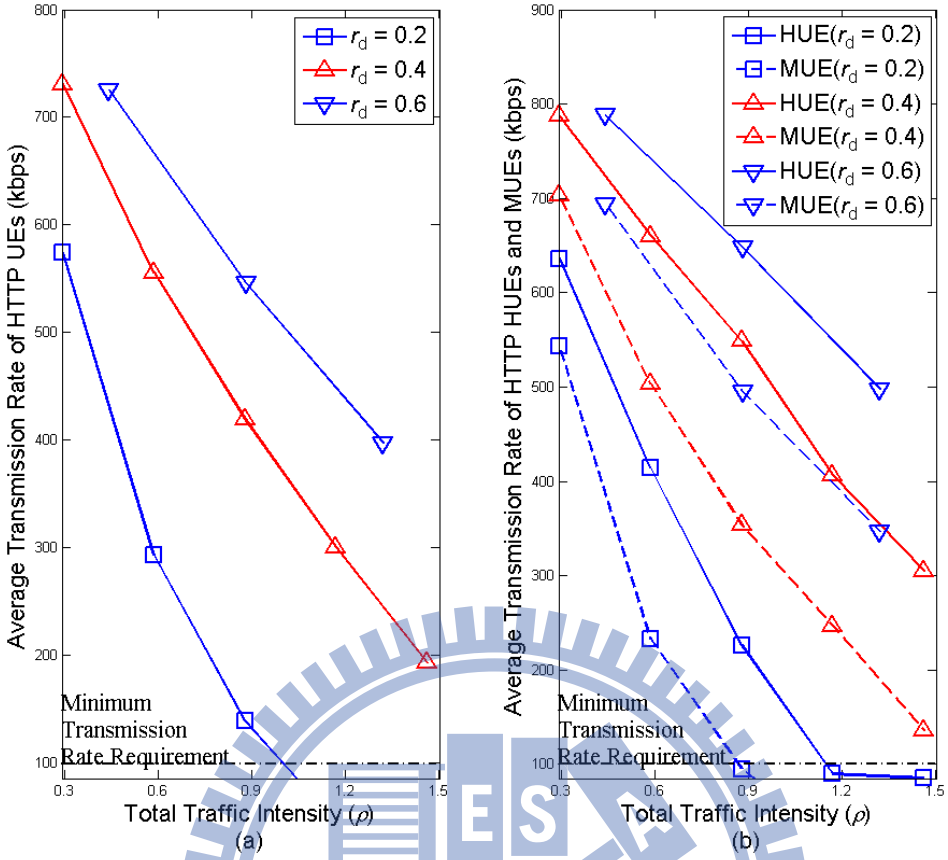

Figure 4.8 (a) Average transmission rate of HTTP UEs, as well as (b) HTTP HUEs and MUEs.

4.5 Performance Evaluation

Since MUEs in the cell-edge region have worse channel condition to MeNB than MUEs in other regions, the cell-edge MUEs are more anxious to be served by the nearby hybrid access HeNBs than MUEs in other regions. Hence, we compare the proposed CPRM scheme with the DBRM and CRRM schemes in two regions, which are the cell-edge region of a sector, and the entire region of a sector. Besides, because the CPRM scheme in r_d of 0.4 can satisfy the QoS requirements of all traffic types in the total traffic intensity of 1.46, and achieve larger throughput than that in r_d of 0.6, when it has sufficient resource to serve all UEs, we set r_d to be 0.4 and evaluate the performance.

4.5.1 Cell-edge region scenario

Figure 4.9 displays the percentage of failed allocation to UEs, and the average sensing duration on total bandwidth in a frame duration. The failed allocation indicates that HeNB cannot transmit the determined bits to UE by the allocated power on the allocated sub-channel at the allocated sub-frames. It can be found that the percentage of failed allocation of CPRM scheme is smaller by more than 69.6% and 70.6%, compared to that of the DBRM and CRRM schemes, when the total traffic intensity exceeds 0.88. Besides, though the DBRM scheme has smaller percentage of failed allocation than the CRRM scheme, its probability of failed allocation increases rapidly as the total traffic intensity increases. However, the CPRM scheme has a decreasing sensing duration as the total traffic intensity increases, while the DBRM and CRRM schemes keep the same constant sensing duration.

The first phenomenon is because the CPRM scheme can adapt the sensing duration on sub-channel to obtain more accurate sensing result than the DBRM and CRRM schemes. The second phenomenon is because the DBRM scheme considers dividing its total power to all UEs, and the CRRM scheme only allocates the required power to transmit the determined transmission bits. Thus, the DBRM scheme would allocate larger or equal power to transmit the same number of bits to UE, compared to the CRRM scheme, under the same sensing result. This makes the DBRM scheme may still be able to transmit the determined bits to UE, even if the sensing result is wrong and makes the CRRM scheme have failed allocation. The third phenomenon is due to the feature that the DBRM scheme allocates power relating to the channel condition of serving UEs served by the same HeNB, and the failed allocation to any serving UE would affect allocations to other UEs more heavily as the total traffic intensity increases. The fourth phenomenon is resulted from that the CPRM scheme adapts the sensing duration on sub-channel inversely proportional to the RSS on

sub-channel, and the larger total traffic intensity would result in more RSS.

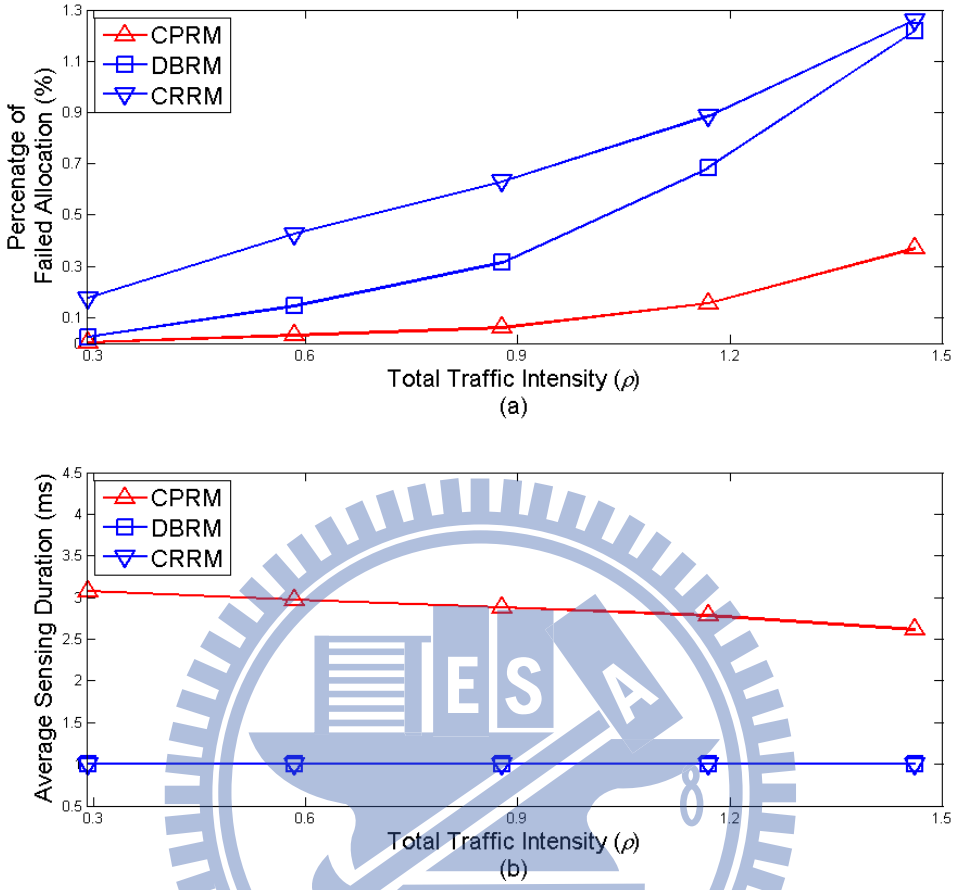

Figure 4.9 (a) Percentage of failed allocation and (b) average sensing duration.

Figure 4.10 demonstrates the throughput of UEs, throughput of HUEs, and throughput of MUEs. We can learn that the throughput of UEs of the CPRM scheme can achieve larger by 4.8% and 14.5%, compared to that of the DBRM and CRRM schemes in the total traffic intensity of 1.46. Besides, in the total traffic intensity of 1.46, the CPRM scheme has obviously larger throughput of HUEs than the DBRM and CRRM schemes by 9.9% and 23.6%, respectively, while it has slightly larger throughput of MUEs than the DBRM and CRRM schemes by 2% and 9.7%, respectively. This result is explained as follows. The CPRM scheme adapts the sensing duration on sub-channels to obtain accurate sensing results, designs the priority function and the minimum transmission bits to UEs to satisfy the QoS

requirements of UEs, and then allocates resource in the descending order of priority to avoid violating QoS requirements of urgent UEs. On the other hand, due to the fact that the DBRM scheme allocates resource based on the channel condition, and the CRRM scheme allocates radio resource regardless of the channel condition, the DBRM scheme can achieve larger system throughput, throughput of HUEs, and throughput of MUEs than the CRRM scheme.

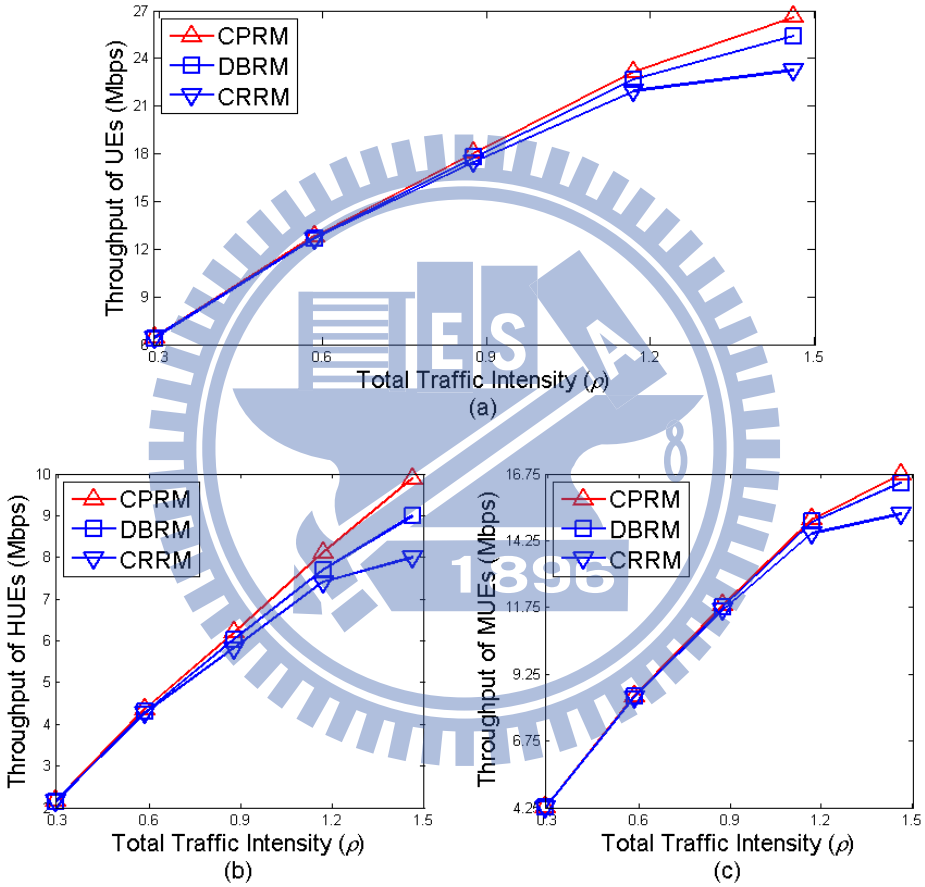

Figure 4.10 (a) Throughput of UEs, (b) throughput of HUEs, and (c) throughput of MUEs.

Figure 4.11 shows the packet dropping rate of voice and video UEs, while Figure 4.12 shows the packet dropping rate of voice HUEs and MUEs, as well as that of video HUEs and MUEs. It can be discovered that the CPRM scheme can still satisfy the packet dropping rate requirement of voice and video UEs in the total traffic

intensity of 1.46. Besides, the DBRM scheme violates the packet dropping rate requirement of voice and video UEs in the total traffic intensity of 1.46 and 1.17, respectively, and the CRRM scheme violates the packet dropping rate requirement of voice and video UEs in the total traffic intensity of 1.46 and 0.88, respectively. This is because the CPRM scheme designs the minimum transmission bits to guarantee the QoS requirements of UEs, the CPRM scheme could prevent that there is insufficient resource when the urgent RT UEs are going to violate the delay tolerance requirement. On the other hand, since the DBRM scheme considers the channel condition, while the CRRM scheme neglects the channel condition, and HUE usually has better channel condition than MUE, the DBRM scheme has lower packet dropping rate of voice and video HUEs than that of the CRRM scheme.

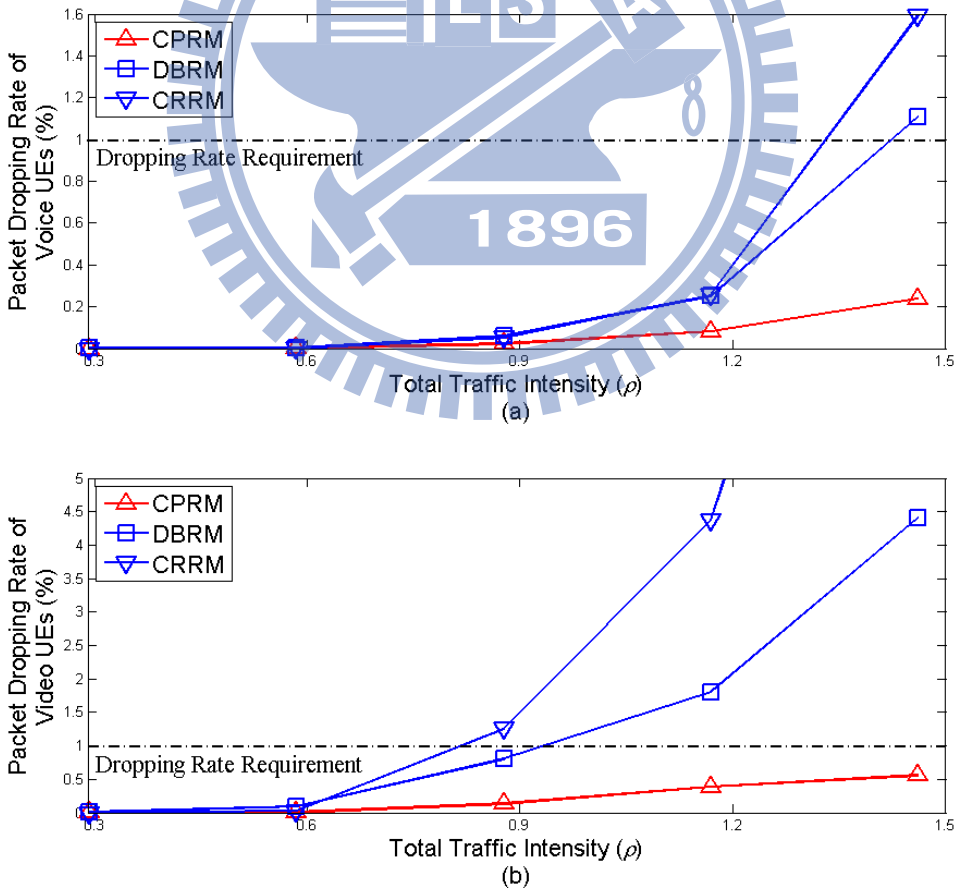

Figure 4.11 Packet dropping rate of (a) voice and (b) video UEs.

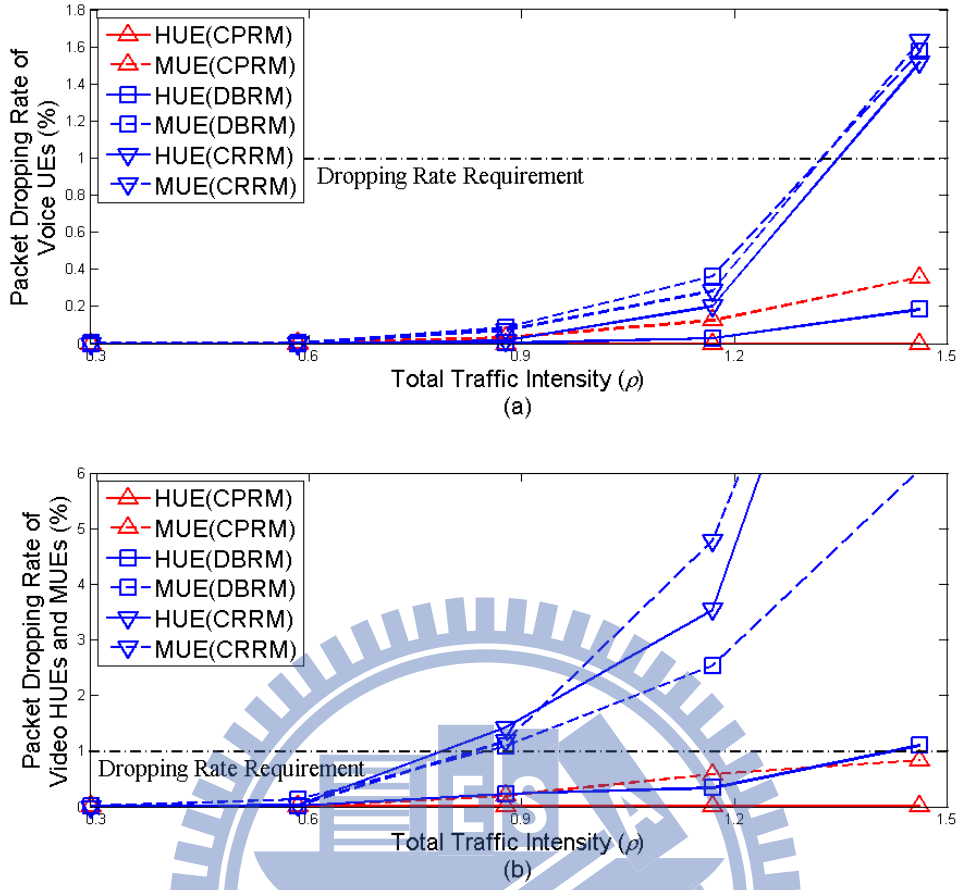

Figure 4.12 Packet dropping rate of (a) voice HUEs and MUEs, as well as (b) video HUEs and MUEs.

Figure 4.13 presents the average packet delay of voice and video UEs, while Figure 4.14 presents the average packet delay of voice HUEs and MUEs, as well as that of video HUEs and MUEs. The CPRM scheme has smaller packet delay of voice and video HUEs than the CRRM scheme as the total traffic intensity exceeds 1.17 and 0.88, respectively. Besides, the CRRM scheme has the smallest packet delay of voice and video UEs, as well as that of voice and video MUEs among the three schemes before the total traffic intensity is 1.46. However, the DBRM scheme has dramatically increasing packet delay of voice and video UEs as the total traffic intensity increase. The first consequence is because there is insufficient resource as the total traffic intensity increases, and the CPRM scheme tends to serve RT HUE prior to other UEs. The second consequence is due to the fact the CRRM scheme considers the delay

tolerance requirements of RT UEs but neglects the channel condition. However, the third consequence is because the DBRM scheme only considers the urgent UE, and thus serves the RT UEs when they have large delay.

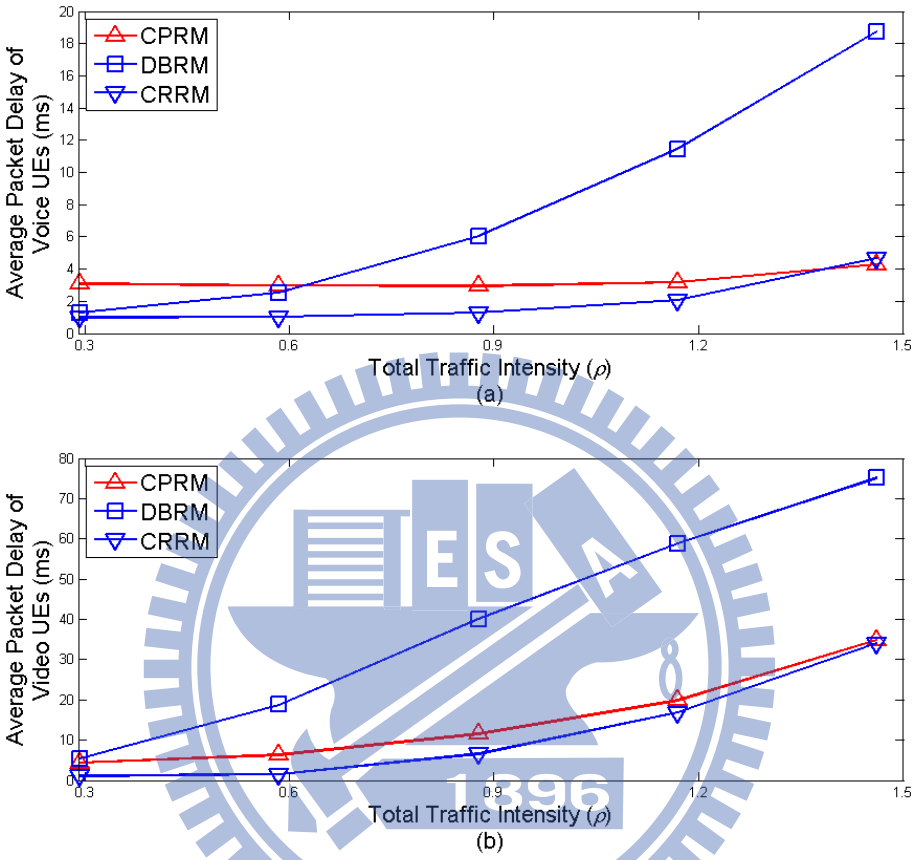

Figure 4.13 Average packet delay of (a) voice and (b) video UEs.

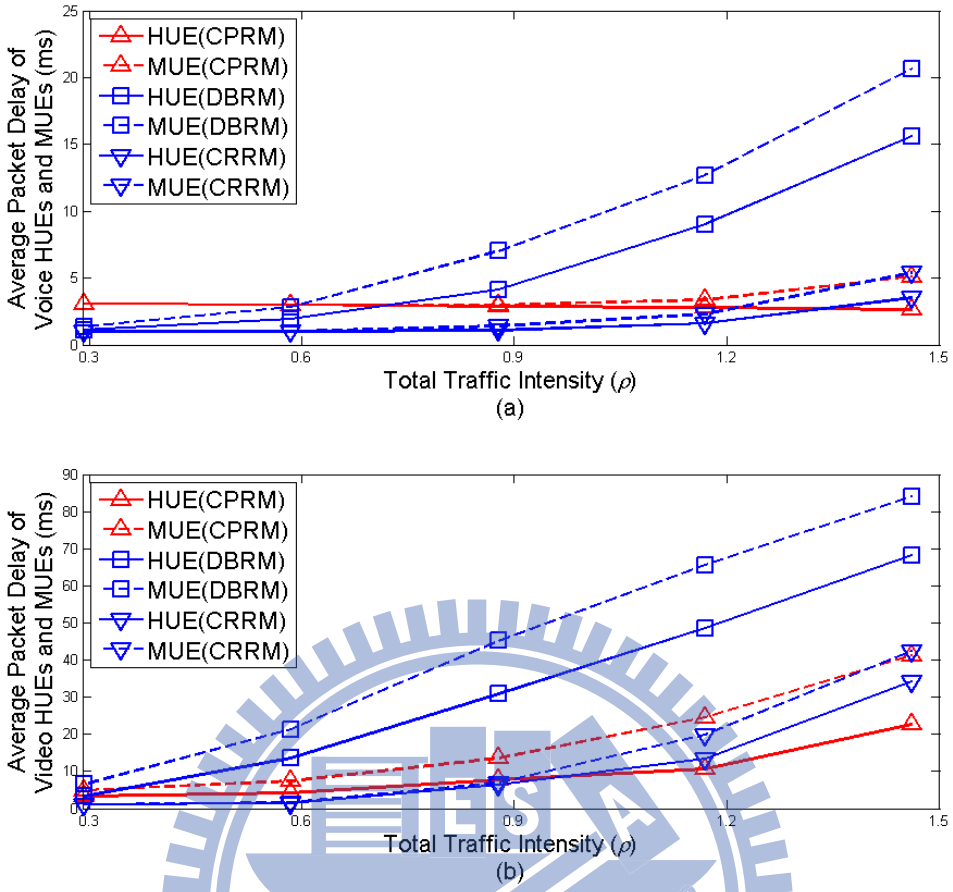

Figure 4.14 Average packet delay of (a) voice HUEs and MUEs, as well as (b) video HUEs and MUEs.

Figure 4.15 illustrates the average transmission rate of HTTP UEs, as well as that of HTTP HUEs and MUEs. We can see that the three schemes can still satisfy the minimum transmission rate requirement of HTTP UEs in the total traffic intensity of 1.46, and the transmission rate of the CPRM scheme is larger by more than 24.2% and 24.7%, compared to that of the DBRM and CRRM schemes, when the total traffic intensity exceeds 0.88. Moreover, the DBRM scheme has smaller transmission rate than the CRRM scheme before the total traffic intensity is 0.88. On the other hand, the CPRM scheme can achieve larger transmission rate of HTTP HUEs than the DBRM and CRRM schemes by more than 38.4% and 35.4%, respectively, and larger transmission rate of HTTP MUEs than the DBRM and CRRM schemes by more than 15.1% and 17.5%, respectively, when the total traffic intensity exceeds 0.88.

The first phenomenon is because all the three schemes consider the urgent HTTP UEs, and the CPRM scheme assigns higher priority to urgent HTTP UE than un-urgent RT UE to guarantee the minimum transmission rate requirement of HTTP UE. The second phenomenon is due to the fact that the CRRM scheme considers the minimum transmission rate requirement of HTTP UEs but neglects the channel condition, and the DBRM scheme only considers the urgent HTTP UE. Besides, there are severer interference and more urgent HTTP UEs as the total traffic intensity increases. The third phenomenon is because the CPRM scheme sets the minimum transmission bits to satisfy the minimum transmission rate of HTTP UE.

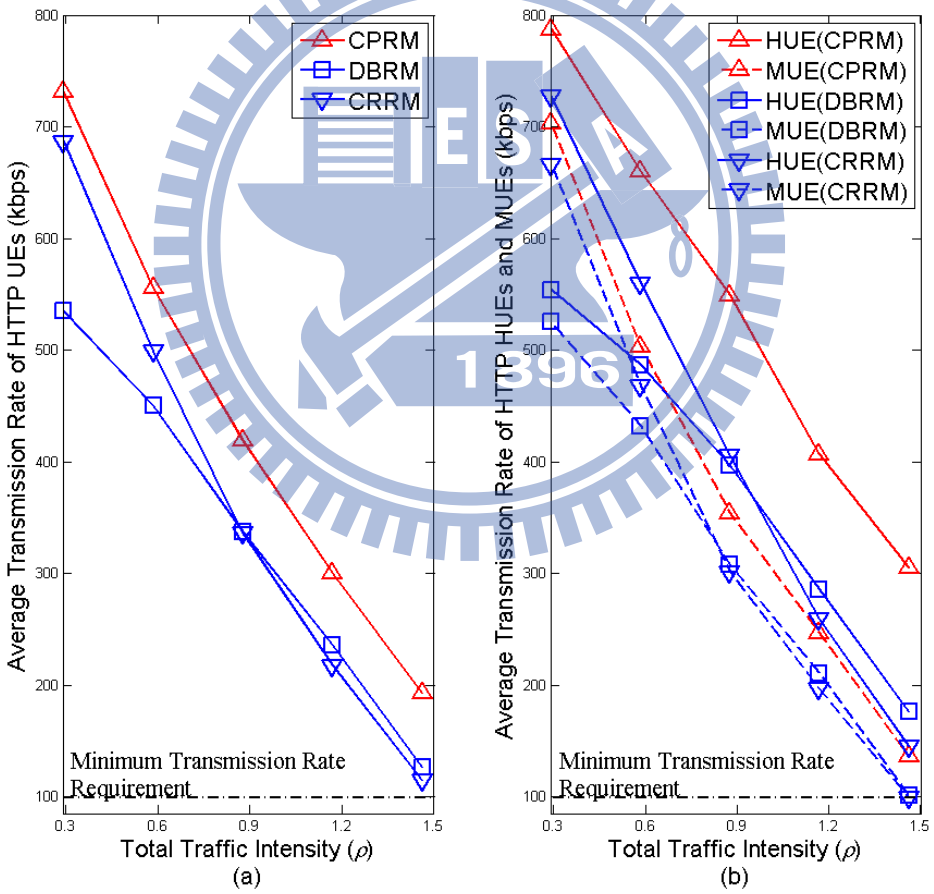

Figure 4.15 (a) Average transmission rate of HTTP UEs, as well as (b) HTTP HUEs and MUEs.

Figure 4.16 depicts the throughput of FTP traffic, throughput of FTP HUEs, and throughput of FTP MUEs. It can be noticed that the throughput of FTP traffic of the CPRM scheme is larger by more than 3.3% and 6.4%, compared to that of the DBRM and CRRM schemes. Besides, the throughput of FTP MUEs of the CPRM, DBRM, and CRRM schemes decreases by 4.7%, 2.9%, and 1.8%, respectively, when the total traffic intensity exceeds 1.17. On the other hand, the throughput of FTP HUEs of the CPRM scheme is larger by more than 10.8% and 15.7%, compared to that of the DBRM and CRRM schemes, when the total traffic intensity exceeds 1.17. However, the throughput of FTP MUEs of the CPRM scheme is smaller by 2.5% and 1.5%, compared to that of the DBRM and CRRM schemes in the total traffic intensity of 1.46.

The first consequence is because there is insufficient resource to serve all UEs, and FTP traffic is a BE service. Besides, since the CPRM and DBRM schemes would allocate resource in the descending order of the channel condition, and MUE usually has worse channel condition than HUE, and thus the CPRM and DBRM schemes have more decrease in the throughput of FTP MUEs as the total traffic intensity increases. The second consequence is due to the fact that there is insufficient resource to serve all UEs as the total traffic intensity exceeds 1.17, and the CPRM scheme assigns the lowest priority to the FTP MUEs, and then it might have no resource to serve FTP MUEs.

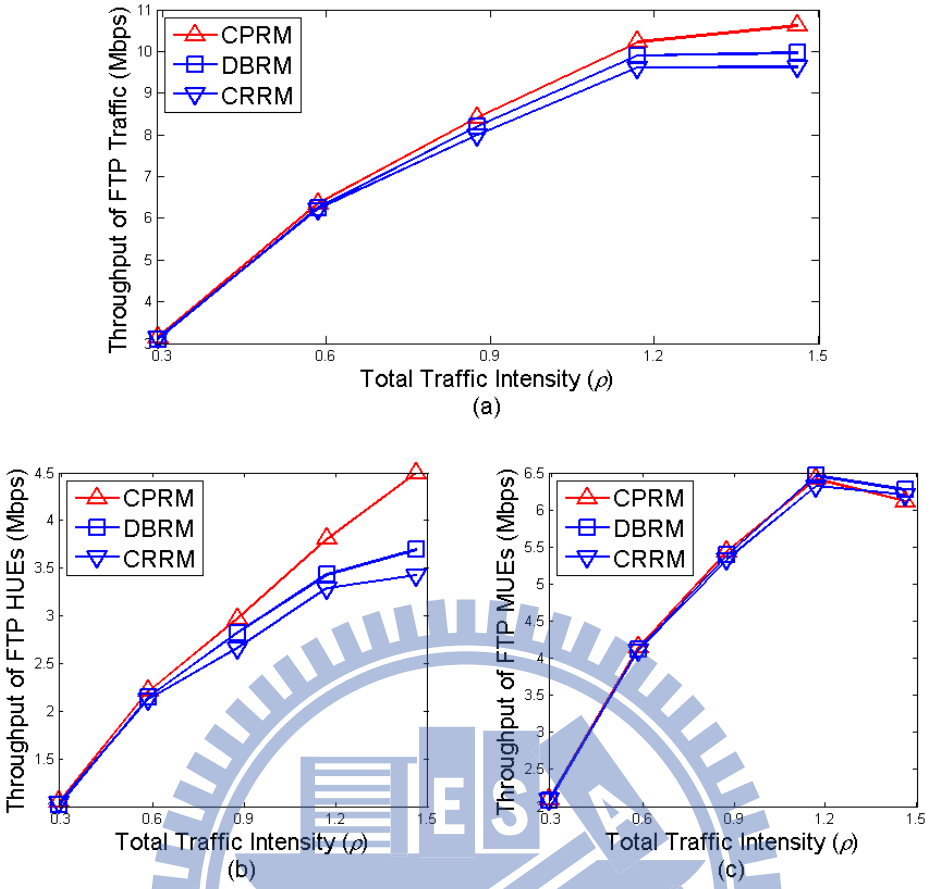

Figure 4.16 Throughput of (a) FTP traffic, (b) FTP HUEs, and (c) FTP MUEs.

4.5.2 Entire region scenario

Figure 4.17 shows the throughput of UEs, throughput of HUEs, and throughput of MUEs. We can see that the throughput of UEs of the CPRM scheme can achieve larger throughput of UEs by 3.8% and 12.6%, compared to that of the DBRM and CRRM schemes in the total traffic intensity of 1.46. Besides, in the total traffic intensity of 1.46, the CPRM scheme has larger throughput of HUEs than the DBRM and CRRM schemes by 10.2% and 22.4%, respectively, while it has slightly larger throughput of MUEs than the DBRM and CRRM schemes by 0.4% and 7.5%, respectively. The reasons are given in Figure 4.10. However, since the hybrid access HeNB has less serving MUEs, when it is not in the cell-edge region, the CPRM scheme has less outperformance in the throughput of MUEs than the conventional schemes in the entire region of a sector.

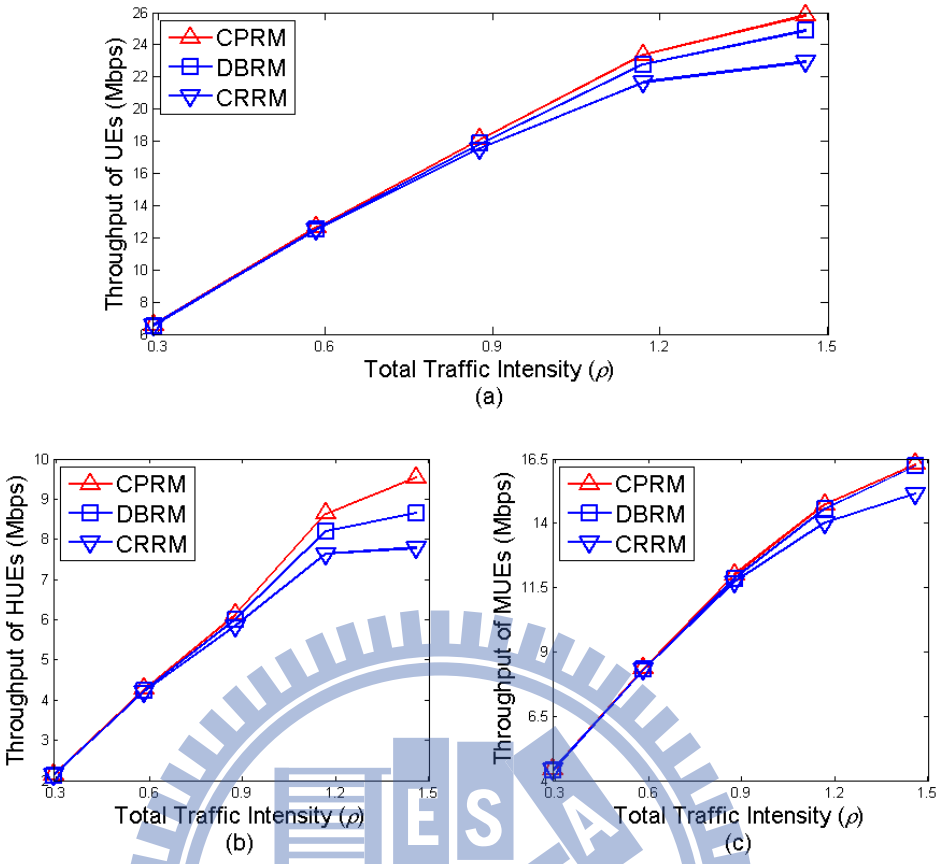

Figure 4.17 (a) Throughput of UEs, (b) throughput of HUEs, and (c) throughput of MUEs.

Figure 4.18 illustrates the packet dropping rate of voice and video UEs. We can discover that the CPRM scheme can still satisfy the packet dropping rate requirement of voice and video UEs in the total traffic intensity of 1.46. Besides, the DBRM scheme violates the packet dropping rate requirement of voice and video UEs in the total traffic intensity of 1.46 and 1.17, respectively, and the CRRM scheme violates the packet dropping rate requirement of voice and video UEs in the total traffic intensity of 1.46 and 0.88, respectively. These phenomena are explained as in Figure 4.11.

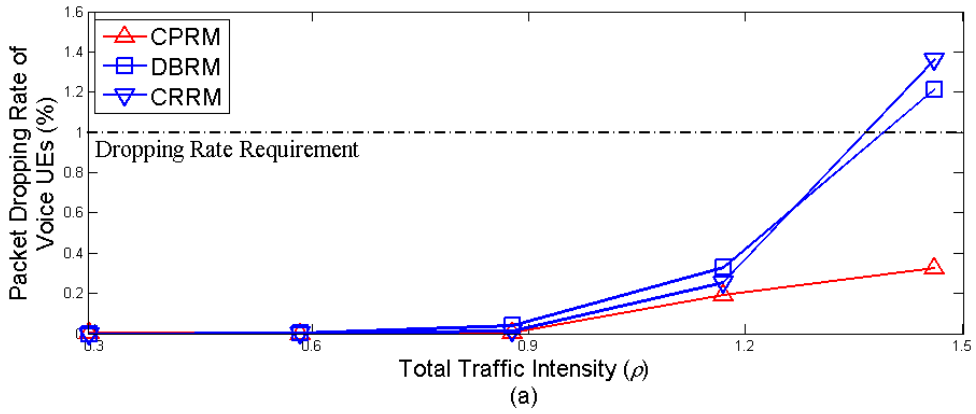

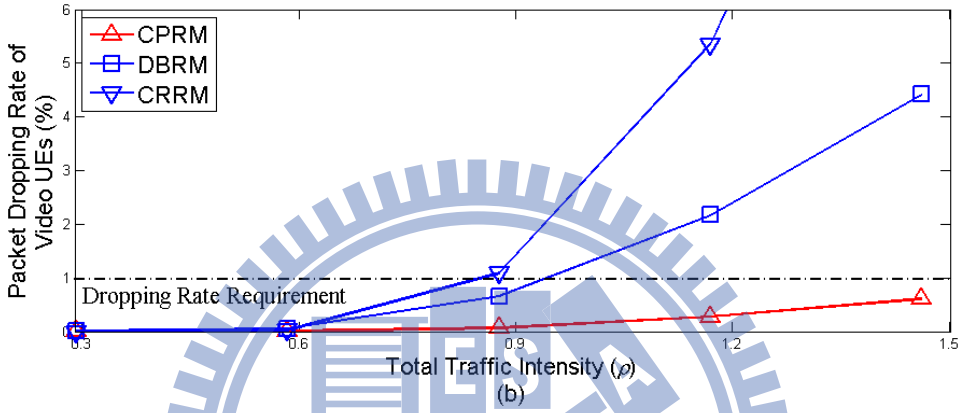

Figure 4.18 Packet dropping rate of (a) voice and (b) video UEs.

Figure 4.19 presents the average packet delay of voice and video UEs. We can notice that the CRRM scheme has the smallest packet delay of voice and video UEs before the total traffic intensity is 1.46, and the CPRM scheme has smaller packet delay of voice and video UEs after then. Besides, the DBRM scheme has dramatically increasing packet delay of voice and video UEs as the total traffic intensity increase. These consequences are explained as in Figure 4.13.

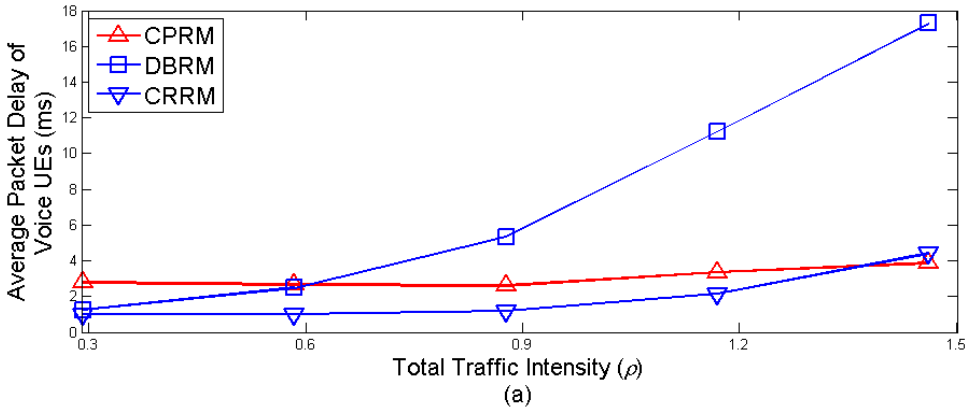

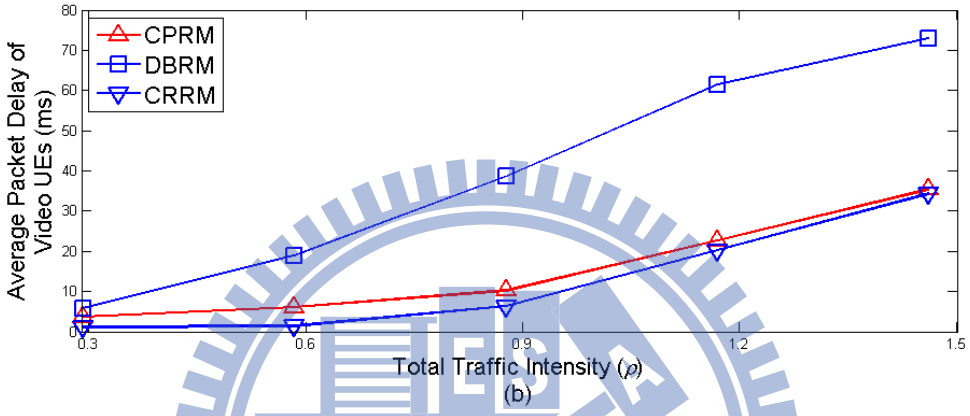

Figure 4.19 Packet dropping rate of (a) voice HUEs and MUEs, as well as (b) video HUEs and MUEs.

Figure 4.20 exhibits the average transmission rate of HTTP UEs. We can find that the three schemes can still satisfy the minimum transmission rate requirement of HTTP UEs in the total traffic intensity of 1.46, and the transmission rate of the CPRM scheme is larger by more than 22.5% and 27.3%, compared to that of the DBRM and CRRM schemes, when the total traffic intensity exceeds 0.88. Moreover, the DBRM scheme has smaller transmission rate than the CRRM scheme before the total traffic intensity is 0.88. Theses phenomena can be discussed as in Figure 4.15 (a).

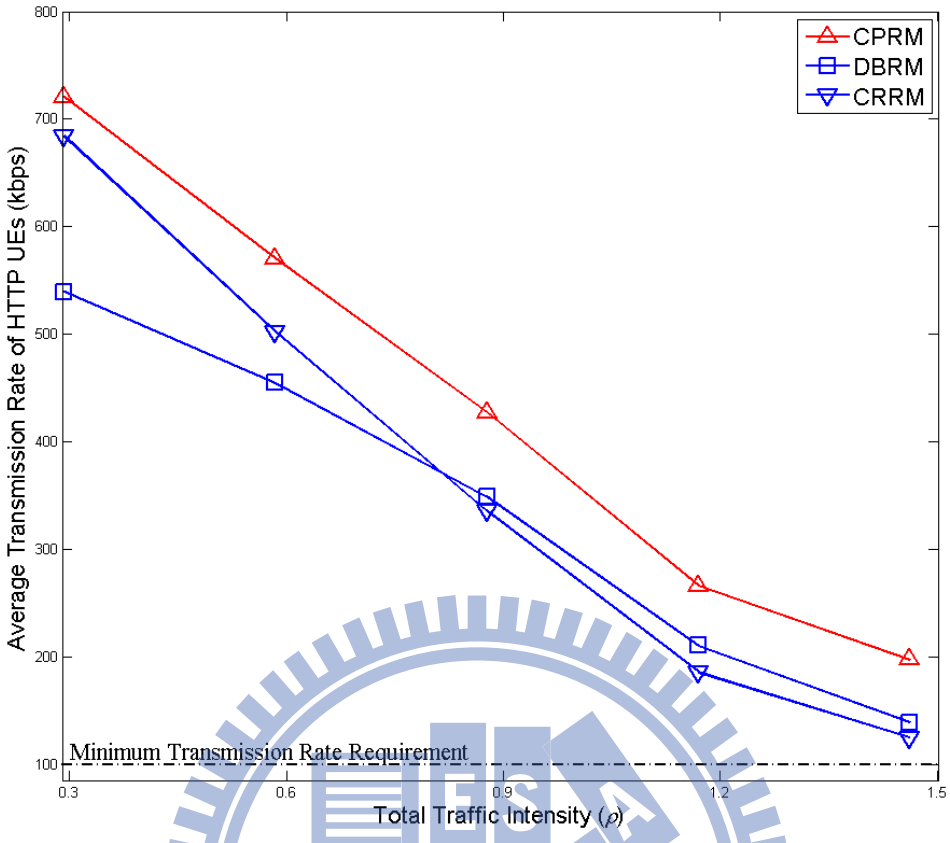

Figure 4.20 Average transmission rate of HTTP UEs.

Figure 4.21 depicts the throughput of FTP traffic, throughput of FTP HUEs, and throughput of FTP MUEs. We can learn that the throughput of FTP traffic of these three schemes decrease as the total traffic intensity exceeds 1.17, and that of the CPRM scheme can be larger by more than 3.6% and 9.7%, compared to that of the DBRM and CRRM schemes, then. Besides, the throughput of FTP HUEs of the CPRM, DBRM, and CRRM schemes decreases by 1.4%, 12.3%, and 7.3%, respectively, when the total traffic intensity exceeds 1.17. On the other hand, the throughput of FTP MUEs of the CPRM scheme is smaller by 6.2% and 7%, compared to that of the DBRM and CRRM schemes in the total traffic intensity of 1.46.

The first consequence is due to the insufficient resource for FTP traffic in the heavy total traffic intensity, and the second one is because there would be more resource for FTP traffic when HeNB is not in the cell-edge region, and then the

CPRM scheme can outperform the DBRM and CRRM schemes more. The third consequence is resulted from the fact that HeNB needs more power to satisfy the QoS requirements of UEs, when it is near the MeNB, and thus it has insufficient resource to serve HUE in the heavy total traffic intensity. The fourth consequence is because the CPRM scheme allocates resource based on the priority, and assigns the lowest priority to the FTP MUEs.

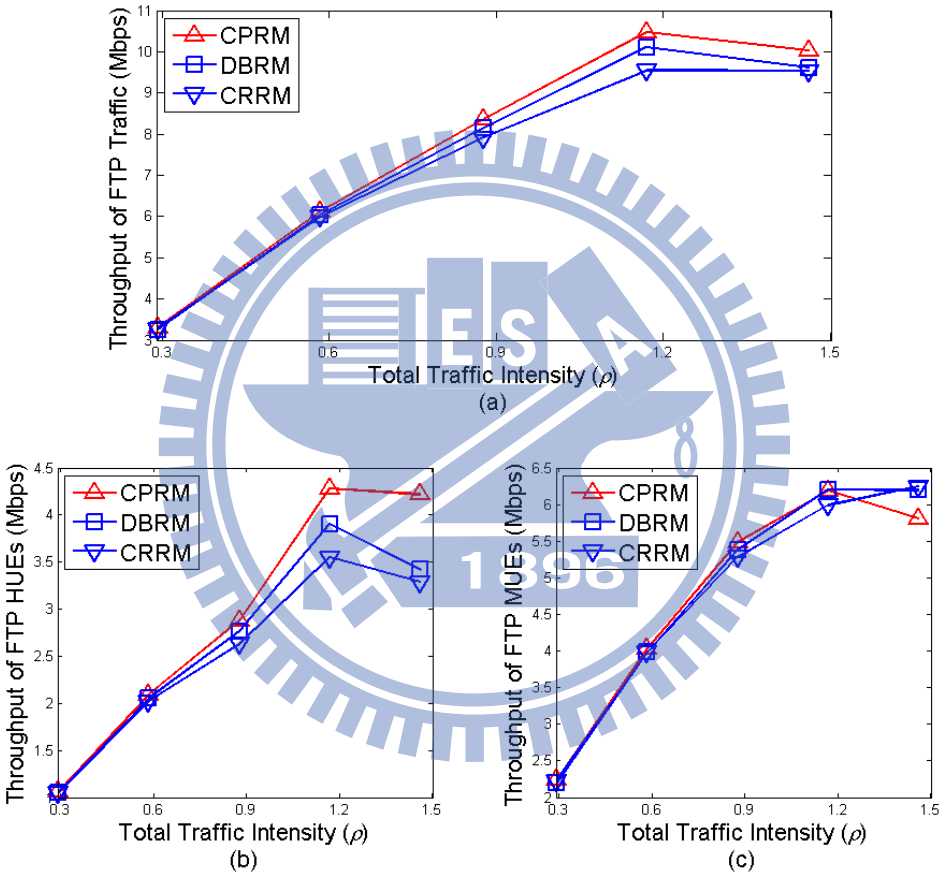

Figure 4.21 Throughput of (a) FTP traffic, (b) FTP HUEs, and (c) FTP MUEs.

Chapter 5

Conclusions

In this thesis, we propose the cognitive priority-based resource management (CPRM) scheme for hybrid access HeNB in the macro-femto networks, while we consider four traffic types so as to analyze the performance of the CPRM scheme in practice. The CPRM scheme is composed of three algorithms: cognitive channel determination (CCD) algorithm, priority and minimum bits determination (PBD) algorithm, and priority-based resource allocation (PRA) algorithm.

The CCD algorithm designs an adaptive sensing duration in the beginning of every frame for sensing the bandwidth accurately, and indicates the set of available sub-channels. Although this makes the CPRM scheme have longer sensing time than the conventional schemes, decomposition-based resource management (DBRM) and cognitive radio resource management (CRRM) schemes, the CPRM scheme achieves smaller percentage of failed allocation than the DBRM and CRRM schemes by more than 69.6% and 70.6%, respectively, when the total traffic intensity exceeds 0.88. The PBD algorithm designs a priority function to indicate the urgency of UE, and determines the minimum number of transmission bits so as to guarantee the QoS requirements of urgent and un-urgent UEs. Besides, the PRA algorithm allocates the best sub-channel to UE in the descending order of priority so as to avoid the urgent UE violating its QoS requirements and maximize the system throughput. However,

the CPRM scheme can achieve larger system throughput than the DBRM and CRRM schemes by 4.8% and 14.5%, respectively, in the total traffic intensity of 1.46.

From the simulation results in Chapter 4, we can conclude that the CPRM scheme outperforms the DBRM and CRRM schemes in maximizing the system throughput of hybrid access HeNB in the cell-edge region of the macro-femto networks with guaranteeing the QoS requirements of all traffic types.

Bibliography

[1] D. Astely, E. Dahlman, A. Furuskar, Y. Jading, M. Lindstrom, and S. Parkvall, "LTE: The Evolution of Mobile Broadband," *IEEE MCOM*, Vol. 47, No. 4, pp. 44-51, Apr. 2009.

[2] I. F. Akyildiz, D. M. Gutierrez-Estevez, and E. C. Reyes, "The Evolution to 4G Cellular Systems: LTE-Advanced," *PHYCOM*, Vol. 3, No. 4, pp. 217-244, Dec. 2010.

[3] 3GPP, "Requirements for Further Advancements for Evolved Universal Terrestrial Radio Access (E-UTRA) (LTE-Advanced)," 3GPP TR 36.913 v10.0.0, 2011.

[4] B. A. Bjerke, "LTE-advanced and The Evolution of LTE Deployments," *IEEE MWC*, Vol. 18, No. 5, pp. 4-5, Oct. 2011.

[5] M. Baker, "From LTE-advanced to The Future," *IEEE MCOM*, Vol. 50, No. 2, pp. 116-120, Feb. 2012.

[6] A. Ghosh, R. Ratasuk, B. Mondal, N. Mangalvedhe, and T. Thomas, "LTE-Advanced: Next-Generation Wireless Broadband Technology," *IEEE MWC*, Vol. 17, No. 3, pp. 10-22, Jun. 2010.

[7] D. Erik, P. Stefan, and S. Johan, *4G: LTE/LTE-Advanced for Mobile Broadband*, Academic Press, 2011.

[8] V. Chandrasekhar, J. Andrews, and A. Gatherer, "Femtocell Networks: A Survey," *IEEE MCOM*, Vol. 46, No.9, pp. 59-67, Sep. 2008.

[9] J. Weitzen, and T. Grosch, "Comparing Coverage Quality for Femtocell and

Macrocell Broadband Data Services," *IEEE MCOM*, Vol. 48, No. 1, pp. 40-44, Jan 2010.

[10] S. F. Hasan, N. H. Siddique,and S. Chakraborty, "Femtocell versus WiFi - A Survey and Comparison of Architecture and Performance," *IEEE WIRELESSVITAE*, pp. 916-920, May. 2009.

[11] A. Golaup, M. Mustapha, and L. B. Patanapongpibul, "Femtocell Access Control Strategy in UMTS and LTE," *IEEE MCOM*, Vol. 47, No. 9, pp. 117-123, Sep. 2009.

[12] G. de la Roche, A. Valcarce, D. Lopez-Perez, and J. Zhang, "Access Control Mechanisms for Femtocells," *IEEE MCOM*, Vol. 48, No. 1, pp. 33-39, Jan. 2010.

[13] D. Lopez-Perez, A. Valcarce, G. de la Roche, and J. Zhang, "OFDMA Femtocells: A Roadmap on Interference Avoidance," *IEEE MCOM*, Vol. 47, No. 9, pp. 41-48, Sep. 2009.

[14] Y. Sun, R.P. Jover, and X. Wang, "Uplink Interference Mitigation for OFDMA Femtocell Networks," *IEEE TWC*, Vol. 11, No. 9, pp. 614-625, Feb. 2012.

[15] V. Chandrasekhar, J. G. Andrews, T. Muharemovic, Z. Shen, and A. Gatherer, "Power Control in Two-tier Femtocell Networks," *IEEE TWC*, Vol. 8, No. 8, pp. 4316-4328, Aug. 2009.

[16] M. Rahman and H. Yanikomeroglu, "Enhancing Cell-edge Performance: A Downlink Dynamic Interference Avoidance Scheme with Inter-cell Coordination," *IEEE TWC*, Vol. 9, No. 4, pp. 1414-1425, Apr. 2010.

[17] H. S. Jo, C. Mun, J. Moon, and J. G. Yook, "Interference Mitigation Using Uplink Power Control for Two-tier Femtocell Networks," *IEEE TWC*, Vol. 8, No. 10, pp. 4906-4910, Oct. 2009.

[18] H. S. Jo, C. Mun, J. Moon, and J. G. Yook, "Self-Optimized Coverage Coordi-

nation in Femtocell Networks," *IEEE TWC*, Vol. 9, No. 10, pp. 2977-2982, Oct. 2010.

[19] X. Chu, Y. Wu, D. Lopez-Perez, and X. Tao, "On Providing Downlink Services in Collocated Spectrum-Sharing Macro and Femto Networks," *IEEE TWC*, Vol. 10, No. 12, pp. 4306-4315, Dec. 2011.

[20] S. Al-Rubaye, A. Al-Dulaimi, and J. Cosmas, "Cognitive Femtocell," *IEEE MVT*, Vol. 6, No. 1, pp. 44-51, Mar. 2011.

[21] A. Attar, V. Krishnamurthy, and O. N. Gharehshiran, "Interference Management Using Cognitive Base-Stations for UMTS LTE," *IEEE MCOM*, Vol. 49, No. 8, pp. 152-159, Aug. 2011.

[22] S. Haykin, "Cognitive Radio: Brain-Empowered Wireless Communications," *IEEE JSAC*, Vol. 23, No. 2, pp. 201-220, Feb. 2005.

[23] G. Gür, S. Bayhan, and F. Alagöz, "Cognitive Femtocell Networks: An Overlay Architecture for Localized Dynamic Spectrum Access," *IEEE MWC*, Vol. 17, No. 4, pp. 62-70, Aug. 2010.

[24] Y. Y. Li, M. Macuha, E. S. Sousa, T. Sato, and M. Nanri, "Cognitive Interference Management in 3G Femtocells," *IEEE PIMRC*, pp. 1118-1122, Sep. 2009.

[25] M. E. Sahin, I. Guvenc, M. R. Jeong and H. Arslan, "Handling CCI and ICI in OFDMA Femtocell Networks through Frequency Scheduling," *IEEE TCE*, Vol. 55, No. 4, pp. 1936-1944, Nov. 2009.

[26] G. W. O. da Costa, A. F. Cattoni, V. A. Roig, and P. E. Mogensen, "Interference Mitigation in Cognitive Femtocells," *IEEE GLOBECOMW*, pp. 721-725, Dec. 2010.

[27] N. Jindal, S. Weber, and J.G. Andrews, "Fractional Power Control for Decentralized Wireless Networks," *IEEE TWC*, Vol. 7, No. 12, pp. 5482-5492,

Dec. 2008.

[28] G. W. O. da Costa, A. F. Cattoni, I. Z. Kovacs, and P. E. Mogensen, "A Scalable Spectrum-Sharing Mechanism for Local Area Network Deployment," *IEEE TVT*, Vol. 59, No. 4, pp. 1630-1645, May. 2010.

[29] S. Y. Lien, C. C. Tseng, K. C. Chen, and C. W. Su, "Cognitive Radio Resource Management for QoS Guarantees in Autonomous Femtocell Networks," *IEEE ICC*, pp. 1-6, May 2010.

[30] S. M. Cheng, S. Y. Lien, F. S. Chu, and K. C. Chen, "On Exploiting Cognitive Radio to Mitigate Interference in Macro/Femto Heterogeneous Networks," *IEEE MWC*, Vol. 18, No. 3, pp. 40-47, Jun. 2011.

[31] S. M. Cheng, W. C. Ao, and K. C. Chen, "Downlink Capacity of Two-tier Cognitive Femto Networks," *IEEE PIMRC*, pp. 1303-1308, Sep. 2010.

[32] J. S. Lin, and K. T. Feng, "Game Theoretical Model and Existence of Win-Win Situation for Femtocell Networks," *IEEE ICC*, pp. 1-5, Jun. 2011.

[33] Y. Yi, J. Zhang, Q. Zhang, and T. Jiang, "Spectrum Leasing to Femto Service Provider with Hybrid Access," *Proceedings IEEE INFOCOM*, pp. 1215-1223, Mar. 2012.

[34] Y. Chen, J. Zhang, Q. Zhang, and J. Jia, "A Reverse Auction Framework for Access Permission Transaction to Promote Hybrid Access in Femtocell Network," *Proceedings IEEE INFOCOM*, pp. 2761-2765, Mar. 2012.

[35] Y. Chen, J. Zhang, and Q. Zhang, "Utility-Aware Refunding Framework for Hybrid Access Femtocell Network," *IEEE MWC*, Vol. 11, No. 5, pp. 1688-1697, May. 2012.

[36] 3GPP, "E-UTRA: Further Advancements for E-UTRA Physical Layer Aspects," 3GPP TR 36.814 v9.0.0, 2010.

[37] 3GPP, "E-UTRA: Physical Channels and Modulation," 3GPP TS 36.211 v10.2.0,

2011.

[38] Y. R. Zheng, and C. Xiao, “Improved Models for The Generation of Multiple Uncorrelated Rayleigh Fading Waveforms,” *IEEE LCOMM*, Vol. 6, No. 6, pp. 256-258, Jun. 2002.

[39] F. Khan, *LTE for 4G Mobile Broadband: Air Interface Technologies and Performance*, Cambridge University Press, 2009.

[40] Y. C. Liang, Y. Zeng, E. C. Y. Peh, and A. T. Hoang, “Sensing-throughput Tradeoff for Cognitive Radio Networks,” *IEEE TWC*, Vol. 7, No. 4, pp. 1326-1337, Apr. 2008.

[41] A. T. Hoang, Y. C. Liang, and Y. Zeng, “Adaptive Joint Scheduling of Spectrum Sensing and Data Transmission in Cognitive Radio Networks,” *IEEE TCOMM*, Vol. 58, No. 1, pp. 235-246, Jan. 2010.

[42] C. F. Tsai, C. J. Chang, F. C. Ren, and C. M. Yen, “Adaptive Radio Resource Allocation for Downlink OFDMA/SDMA Systems with Multimedia Traffic,” *IEEE TWC*, Vol. 7, No. 5, pp. 1734-1743, May. 2008.

[43] J. Xiang, Y. Zhang; T. Skeie, and L. Xie, “Downlink Spectrum Sharing for Cognitive Radio Femtocell Networks,” *IEEE JSYST*, Vol. 4, No. 4, pp. 524-534, Dec. 2010.

[44] S. Y. Lien, Y. Y. Lin, and K. C. Chen, “Cognitive and Game-Theoretical Radio Resource Management for Autonomous Femtocells with QoS Guarantees,” *IEEE TWC* , Vol. 10, No. 7, pp. 2196-2206, Jul. 2011.

Vita

Chang-Cing Ye was born in 1989 in Ilan, Taiwan. He received the B.E. and M.E. degree in Department of Communication Engineering from National Chiao-Tung University, Hsinchu, Taiwan, in 2011 and 2012, respectively. His research interests include wireless communication systems and radio resource management.